



OPEN ACCESS

EDITED BY

Frank Chidawanyika,
International Centre of Insect Physiology and
Ecology (ICIPE), Kenya

REVIEWED BY

Inusa Jacob Ajene,
International Centre of Insect Physiology and
Ecology (ICIPE), Kenya
Casper Nyamukondiwa,
Botswana International University of Science
and Technology, Botswana

*CORRESPONDENCE

Anna Jirošová
✉ jirosovaa@fld.czu.cz

†These authors have contributed equally to
this work

RECEIVED 02 May 2023

ACCEPTED 19 December 2023

PUBLISHED 11 January 2024

CITATION

Ramakrishnan R, Roy A, Hradecký J, Kai M,
Harant K, Svatoš A and Jirošová A (2024)
Juvenile hormone III induction reveals key
genes in general metabolism, pheromone
biosynthesis, and detoxification in Eurasian
spruce bark beetle.
Front. For. Glob. Change 6:1215813.
doi: 10.3389/ffgc.2023.1215813

COPYRIGHT

© 2024 Ramakrishnan, Roy, Hradecký, Kai,
Harant, Svatoš and Jirošová. This is an open-
access article distributed under the terms of
the [Creative Commons Attribution License
\(CC BY\)](https://creativecommons.org/licenses/by/4.0/). The use, distribution or reproduction
in other forums is permitted, provided the
original author(s) and the copyright owner(s)
are credited and that the original publication
in this journal is cited, in accordance with
accepted academic practice. No use,
distribution or reproduction is permitted
which does not comply with these terms.

Juvenile hormone III induction reveals key genes in general metabolism, pheromone biosynthesis, and detoxification in Eurasian spruce bark beetle

Rajarajan Ramakrishnan^{1†}, Amit Roy¹, Jaromír Hradecký¹,
Marco Kai², Karel Harant³, Aleš Svatoš^{2,4} and Anna Jirošová^{1*†}

¹Faculty of Forestry and Wood Sciences, Czech University of Life Sciences Prague, Prague, Czechia, ²Max Planck Institute for Chemical Ecology, Jena, Germany, ³Laboratory of Mass Spectrometry, BIOCEV, Faculty of Science Charles University in Prague, Prague, Czechia, ⁴Institute of Organic Chemistry and Biochemistry, Czech Academy of Sciences, Prague, Czechia

Introduction: In recent years, bark beetle *Ips typographus*, has caused extensive damage to European Norway spruce forests through widespread outbreaks. This pest employs pheromone-assisted aggregation to overcome tree defense, resulting in mass attacks on host spruce. Many morphological and behavioral processes in *I. typographus* are under the regulation of juvenile hormone III (JH III), including the biosynthesis of aggregation pheromones and associated detoxification monoterpene conjugates.

Objectives and Methods: In this study, we topically applied juvenile hormone III (JH III) and performed metabolomics, transcriptomics, and proteomics in *I. typographus* both sexes, with focused aims; 1. Highlight the JH III-regulated metabolic processes; 2. Identify pheromone biosynthesis-linked genes; and 3. Investigate JH III's impact on detoxification conjugates linked to pheromonal components.

Results: Numerous gene families were enriched after JH III treatment, including genes associated with catalytic and oxidoreductase activity, esterases, phosphatases, and membrane transporters. Sex-specific enrichments for reproduction-related and detoxification genes in females and metabolic regulation genes in males were observed. On the protein level were enriched metal ion binding and transferase enzymes in male beetles. After JHIII treatment, mevalonate pathway genes, including terminal isoprenyl diphosphate synthase (IPDS), were exclusively 35- folds upregulated in males, providing evidence of *de novo* biosynthesis of pheromone components 2-methyl-3-buten-2-ol and ipsdienol. In addition, cytochrome P450 genes likely involved in the biosynthesis of *cis/trans*-verbenol, detoxification, and formation of ipsdienol, were 3-fold upregulated in the male gut. The increase in gene expression correlated with the heightened production of the respective metabolites. Detoxification conjugates, verbenyl oleate in the beetle fat body and verbenyl diglycosides in the gut, were induced by JHIII application, which confirms the hormone regulation of their formation. The JH III induction also increased the gene contigs esterase and glycosyl hydrolase up to proteins from male gut tissue. The esterase was proposed to release pheromone *cis*-verbenol in adult males by breaking down verbenyl oleate. The correlating analyses confirmed a reduction in the abundance of verbenyl oleate in the induced male beetle.

Conclusion: The data provide evidence of JH III's regulatory role in the expression of genes and enzymes related to fundamental beetle metabolism, pheromone biosynthesis, and detoxification in *Ips typographus*.

KEYWORDS

Ips typographus, juvenile hormone III, hormonal regulation, mevalonate pathway, CyP450, esterase, monoterpenyl diglycosides, isoprenyl di phosphate synthase

1 Introduction

The Eurasian Spruce Bark Beetle (*Ips typographus*, Coleoptera: Curculionidae) is a pest that severely affects Norway spruce (*Picea abies*) survival across Eurasia (Ward et al., 2022). In recent years, changing climate patterns resulting in extended periods of drought, along with human-induced factors such as establishing monoculture spruce tree plantations, have played a role in exacerbating its outbreaks (Hlasny et al., 2021). In the Czech Republic, from 2018 till 2022, over 50 million m³ of spruce forest have been recorded with bark beetle-infested wood (Knizek et al., 2023). In Europe as a whole, *I. typographus* has killed twice as many trees in the past decade, approximately 70.1 million m³ of timber, nearly all of it Norway spruce (Patacca et al., 2023).

In the class Insecta, many morphological and behavioral changes, such as body development, reproduction, parental care, mating behavior, molt and growth, diapause, and many other functions are hormonally regulated (Jindra et al., 2013; Smykal et al., 2014). The two most important classes of insect hormones are ecdysteroids and juvenile hormones (Pandey and Bloch, 2015). In Coleoptera pheromone biosynthesis concepts, juvenile hormone III (JH III) is the most studied (Keeling et al., 2016). The primary function of these hormones is to maintain juvenile characteristics and prevent premature metamorphosis (Goodman and Cusson, 2012). JH III is synthesized in the exocrine gland corpus allatum and transported through the hemolymph by binding proteins to its target receptors (Jindra and Bittova, 2020). JH III has been extensively used to study many gene families involved in insect growth and metamorphosis, along with social behavior (Riddiford et al., 2010; Trumbo, 2018).

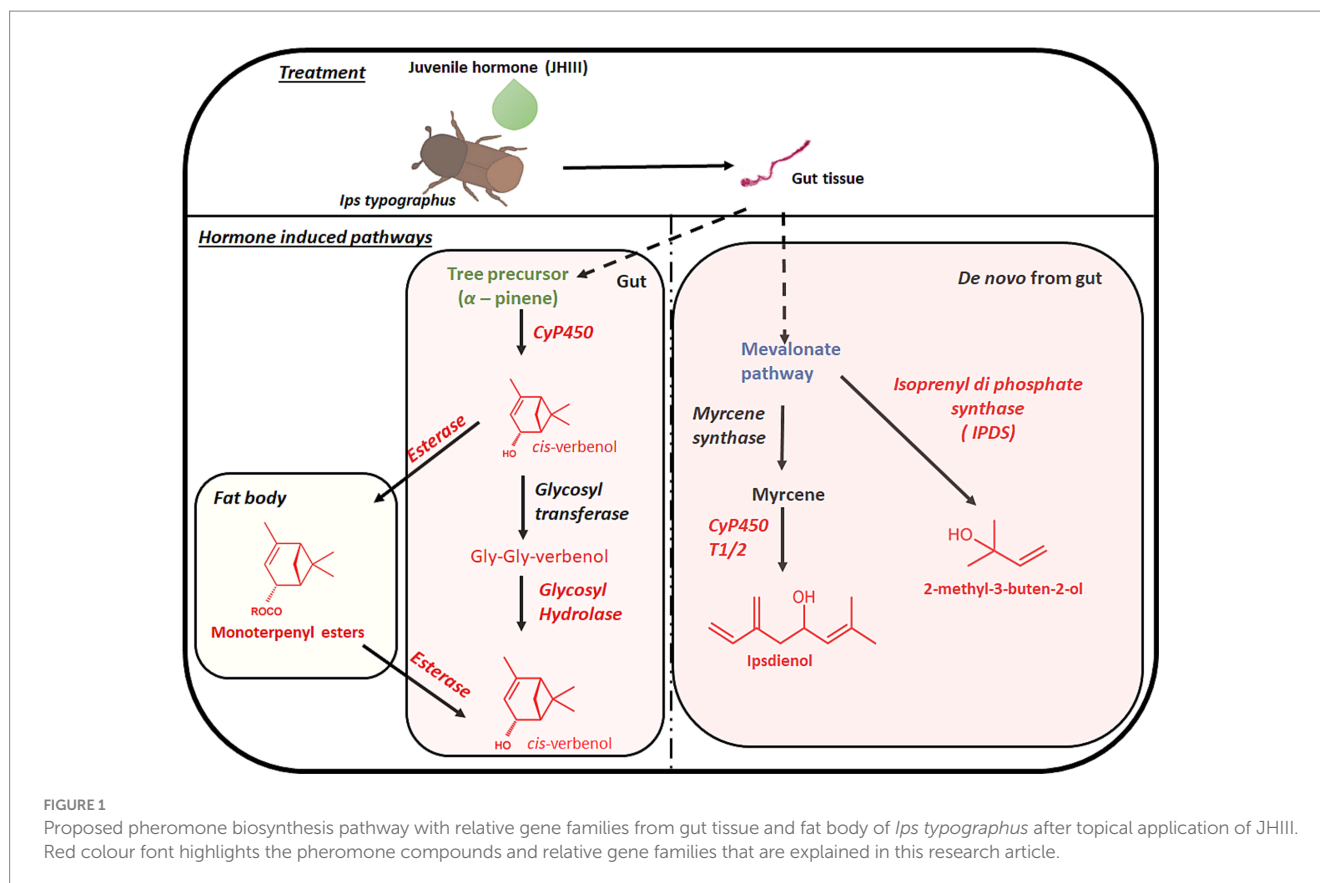
First instar insect larvae initially contain a high titer of JH III, which is subsequently reduced as, the larvae undergo metamorphosis into pupae (Treiblmayr et al., 2006). In the pre-metamorphic stages, JH III has been studied for its influence on the development of larval muscles and the prothoracic glands producing ecdysteroids, as well as its role in restructuring gut development, fat body, and epidermis in various insect species (Riddiford et al., 2001; Riddiford, 2012; Jindra et al., 2013). In the adult insects, JH III influences various aspects, including pheromone production (Tillman et al., 2004) and social behavior (Trumbo, 2018), caste determination (Cristino et al., 2006); aggression and display (Emlen et al., 2006), migration (Zhu et al., 2009), and neuronal remodeling (Leinwand and Scott, 2021).

In bark beetles, JH III effects have primarily been studied in relation to pheromone biosynthesis induction. When the beetles bore into the host tree, JH III is released from the endocrine gland, initiating a series of hormonal signaling processes that lead to the production of aggregation pheromone components in male beetles (Bakke et al., 1977; Schlyter et al., 1987). In nature, this potent blend attracts conspecifics, both males and females, to mass attack to help overcome

tree defense. In controlled laboratory conditions, pheromone biosynthesis induction can be achieved by topically applying JH III on the beetle abdomen (Byers and Birgersson, 1990; Ivarsson et al., 1993; Seybold et al., 1995; Tillman et al., 1998). This method triggers the *de novo* synthesis of pheromone compounds while avoiding potential interference with the metabolic pathways involved in the digestion of ingested phloem tissues. Pheromone induction using JH III has been demonstrated in bark beetles such as *Ips pini*, *Dendroctonus ponderosae*, and *Ips typographus* (Nardi et al., 2002; Tillman et al., 2004; Zhang et al., 2017; Fang et al., 2021a,b; Ramakrishnan et al., 2022a). However, certain *Ips* species such as *I. confusus* and *Ips grandicollis*, have been reported to be unresponsive to JH III-induced pheromone induction (Tillman et al., 2004; Bearfield et al., 2009).

The molecular-level effects of JH III on pheromone biosynthesis have been subsequently investigated in various species, including *Ips paraconfusus* (Ivarsson and Birgersson, 1995), *Ips pini* (Tillman et al., 1998; Blomquist et al., 2010), and *Dendroctonus ponderosae* (Keeling et al., 2016). JH III induction has been found to activate multiple gene families responsible for pheromone biosynthesis, especially in the mevalonate pathway (Sarabia et al., 2019).

In *I. typographus*, male pioneer beetles produce aggregation pheromone blends made up of several terpenoid compounds 2-methyl-3-buten-2-ol, *cis*-verbenol and minor amount of ipsdienol, after successfully boring into the tree bark. Both 2-methyl-3-buten-2-ol and ipsdienol are synthesized in beetle guts through the mevalonate pathway (Figure 1; Ramakrishnan et al., 2022a). In the context of bark beetle pheromone biosynthesis, previous studies have identified key enzymes in the pathway (Tillman et al., 1998). The pathway involves the condensation of acetoacetyl-CoA with acetyl-CoA catalyzed by 3-hydroxy-3-methyl glutaryl coenzyme-A synthase (HMG-S), followed by a reduction of hydroxymethyl glutaryl-CoA to mevalonate, catalyzed by 3-hydroxy-3-methyl glutaryl coenzyme-A reductase (HMG-R). Later, the mevalonate is phosphorylated by phosphomevalonate kinase (PMK), followed by several steps of modification to form the isoprenoid biosynthetic units, isopentenyl diphosphate and dimethyl allyl diphosphate (Buhaescu and Izzedine, 2007). Condensation of two isoprenoid units catalyzed by geranyl diphosphate synthase (GPPS) synthesizes geranyl diphosphate, the precursor of bark beetle monoterpenoid pheromones, such as myrcene and ipsdienol (Gilg et al., 2005; Keeling et al., 2006; Bearfield et al., 2009; Ramakrishnan et al., 2022a). In *I. typographus*, a gene was recently reported that likely encodes an isoprenyl-diphosphate synthase (IPDS) responsible for converting dimethylallyl diphosphate into 2-methyl-3-buten-2-ol, a transformation unique in insects (Ramakrishnan et al., 2022a). Ipsdienol biosynthesis also involves the oxidation of myrcene catalyzed by the cytochrome P450 enzyme CyP450T1/T2 (Sandstrom et al., 2006).



The third pheromonal component in *I. typographus*, *cis*-verbenol, is not synthesized *de novo* but is instead produced through the CyP450 catalyzed oxidation of (–)- α -pinene that adult beetles sequester from the tree (Renwick et al., 1976; Chiu et al., 2019). Additionally, a substantial amount of *cis*-verbenol has been detected in the gut of immature beetles that develop inside the bark, which is believed to be a result of detoxification of toxic α -pinene by these juvenile beetles (Ramakrishnan et al., 2022a). As part of this detoxification process, *cis*-verbenol (along with myrtenol as another detox product) is deposited in the form of monoterpenyl fatty acid esters in the fat body (Chiu et al., 2018; Ramakrishnan et al., 2022a). These conjugates can be hydrolyzed to provide free *cis*-verbenol in adult males when a supply of this pheromonal component is needed. In *I. typographus*, a candidate gene encoding a carboxylesterase (fatty acyl transferase) for the formation of verbenyl oleate (a fatty acid ester) in juvenile beetles was proposed and another carboxylesterase with ester bond cleaving function was suggested to be present in adult males (Ramakrishnan et al., 2022a,b). Another *cis*-verbenol conjugates, created through diglycosylation, has recently been discovered in the gut tissues of *I. typographus* (Ramakrishnan et al., 2022a). Detoxification via glycosylation is a common feature in insects (Hilliou et al., 2021), with UDP-glycosyltransferases being commonly studied as detoxification enzymes (Dai et al., 2021; Powell et al., 2021). In *I. typographus*, *cis*-verbenyl diglycosylate has been proposed as a potential parallel reservoir for the pheromone *cis*-verbenol released by adult males, a hypothesis that aligns with early hypotheses in *D. ponderosae* (Hughes, 1974; White et al., 1980). The effect of JH III on the formation of these detoxification conjugates or cleavage into pheromone-precursors has not been studied yet.

To learn more about the effect of JH III on bark beetle metabolism, we topically applied JH III to *I. typographus* and analyzed changes at the levels of gene transcripts, proteins, and metabolites in both sexes. The primary tissue studied was the gut, the site of pheromone biosynthesis and detoxification.

We hypothesize that JH III will induce correlated changes in genes, proteins and metabolites that reflect the requirements of adult beetles to aggregate and overcome the defense of their host trees by feeding on the phloem and reproduce. These changes are expected to occur in a sex-specific fashion. We also hypothesize that JH III will induce pheromone biosynthesis and the detoxification of spruce defense metabolites, especially those involved in the formation of aggregation pheromones.

By checking the above-mentioned hypothesis, genetic-level research of the bark beetle, *I. typographus* can lead to practical implications using RNA interference silencing of targeted genes and influence the pheromone metabolism. The RNAi technique for Coleopteran (wood-boring) insects has proven for highly susceptible and demonstrated recently on insects such as Emerald ash borer, Asian longhorn beetles, Chinese White pine beetle and Mountain pine beetle (Rodrigues et al., 2017; Dhandapani et al., 2020; Kyre et al., 2020).

2 Materials and methods

2.1 Beetle rearing

Spruce logs (*Picea abies*) naturally infested with *I. typographus* were collected from the Czech University of Life Sciences, Forest

Enterprise in Kostelec and Černými lesy, Czech Republic. The infested logs were stored in a cold chamber (4°C) until further use. The fresh spruce logs (approximately 50 cm) were infested with F0 generation beetles (150 beetles per log) and maintained under laboratory conditions (70% humidity, 24°C, 16:8 h day/night period, and ventilated plastic containers of 56 × 39 × 28 cm/45 L volume) for incubation to establish the F1 generation. After 4 weeks of incubation, F1-generation beetles were collected and sorted for male and female beetles. Subsequently, the beetles were treated with 0.5 µL of acetone (control) or 0.5 µL of a solution of 20 µg/µL JH III in acetone (10 µg of JH III) topically on the abdomen of the beetles. After application, the beetles were kept under laboratory conditions for 8 h. Beetles were frozen in liquid nitrogen and stored at -80°C until further use. Before analysis, the guts were dissected from stored frozen beetles for further downstream analysis. In this study, the beetle body refers to the tissue with fat remaining after removing the gut, elytra, and wings (Ramakrishnan et al., 2022a,b).

2.2 Metabolome

2.2.1 Gas chromatographic-mass spectrometry analysis

The frozen beetles were dissected to extract their guts, which were then placed in 2 mL analytical vials containing 100 µL of cold pentane (10 guts per vial). The beetle bodies were placed in separate vials containing 1 mL of chloroform (10 beetle bodies per vial). The extracts are obtained after overnight incubation at 4°C and tissue free solvents were separated using a short centrifuge (4,000 rpm, 30s) and used for injection.

A Pegasus 4D GC×GC-MS system (LECO, St. Joseph, MI, USA) employing an Agilent 7,890 B and a consumable-free modulator was used to analyze the samples. One microliter of the extract was injected into a cold PTV injector (20C) in split mode at a ratio of 1:3. After injection, the inlet was heated to 275°C at a rate of 8°C/s. Separation was conducted on an HP-5MS UI capillary column (30 m, 0.25 mm i.d., 0.25 µm film thickness, Agilent) coupled to BPX-50 (1.2 m, 0.1 mm i.d., 0.1 µm film thickness, SGE). The GC oven temperature program was as follows: 40°C for 2 min; then ramped at a rate of 10°C min⁻¹ to 200°C; then at 5°C min⁻¹ to 320°C and held for 15 min. The second-dimension oven modulator had offsets of 5°C and 15°C, respectively. The modulation period was 5 s. The total GC runtime was 57 min. Ions (ionization energy of 70 eV) were collected in the mass range of 35–500 Da at a frequency of 100 Hz.

Automated spectral deconvolution and peak-finding algorithms were applied using ChromaTOF software (LECO, St. Joseph, MI, USA). For identification of the compounds, the mass spectra and retention indexes from the National Institute of Standards and Technology (NIST, 2017) mass spectral customized library were used. In the case of fatty acid ester (oleate) was identified using a targeted search using mass spectra and retention indexes obtained from synthetic standards (Chiu et al., 2018) measured under same conditions as in our previous studies (Ramakrishnan et al., 2022a). Relative abundances were defined as the percentage of the peak area of the targeted metabolite in relation to the sum of peak areas of all peaks in the chromatogram.

2.2.2 Ultra-high-performance liquid chromatography-electrospray ionization -high-resolution tandem mass spectrometry analysis

The polar fraction of guts was extracted by adding methanol, water, and acetic acid in a ratio of 70/30/0.5 (v/v) at a volume of 7 mL per gut. The mixture contained ¹³C₂-myristic acid (1 µg/mL) as an internal standard. The gut tissue was sonicated on ice for 5 min and disrupted using a pre-chilled Eppendorf tip. The samples were then centrifuged at 4000 RPM for 3 min, and the supernatant collected in a new vial with a 100 µL glass insert. The polar fractions of gut extracts were subjected to UHPLC-HRMS/MS analysis.

UHPLC-ESI-HRMS/MS was performed using an Ultimate 3,000 series RSLC system (Dionex) coupled to a Q-Exactive HF-X mass spectrometer (Thermo Fisher Scientific). Solvents A-water and B-acetonitrile (LiChrosolv hyper grade for LC-MS; Merck, Darmstadt, Germany), both with 0.1% v/v formic acid (eluent for LC-MS, Sigma Aldrich, Steinheim, Germany), were used for the binary solvent system. 10 µL of the extract was injected, and chromatographic separation was performed with a constant flow rate of 300 µL/min using an Acclaim C18 column (150 × 2.1 mm, 2.2 µm; Dionex, Borgenteich, Germany). Solvent gradients (B 0.5–100% v/v for 15 min; 100% B for 5 min; 100–0.5% v/v for 0.1 min; 0.5% for 5 min) were used. Ionization in the HESI ion source was achieved by 4.2 kV cone voltage, 35 V capillary voltage, and 300°C capillary temperature in the transfer tube in positive ion mode and 3.3 kV cone voltage, 35 V capillary voltage, and 320°C capillary temperature in negative mode. Mass spectra were recorded in both modes at a mass range of m/z 80–800 in duplicate. The obtained fragments with retention time values were interpreted using XCALIBUR software (Thermo Fisher Scientific, Waltham, United States; Ramakrishnan et al., 2022a,b). Metabolite samples were compared and statistically evaluated using MetaboAnalyst 4.0, and the determined masses were compared with the database (Chong et al., 2018). The amounts of three diglycosides of oxygenated monoterpenes (verbenol) were determined with mass spectra obtained from our previous work (Ramakrishnan et al., 2022b).

2.3 Transcriptome

2.3.1 Sample preparation

The beetle guts were dissected in RNAlater. Four biological replicate included three technical replicates each containing 10 pooled guts was used. Total RNA was extracted from male gut tissue samples using a pre-optimized protocol (Sellamuthu et al., 2022) and sent for sequencing with a NOVAseq6000 (PE150, 30 million raw reads) after quality determination using an agarose gel and a bioanalyzer. RNA (1 µg) was used for cDNA synthesis using the M-MLV reverse transcriptase kit following the manufacturer's protocol and stored at -80°C for downstream analysis.

2.3.2 Differential gene expression analysis

RNA-seq. Data were analyzed using CLC workbench 21.0.5 (QIAGEN Aarhus, Denmark) with a pre-optimized setting for mapping exon regions with genome reference (Naseer et al., 2023). Furthermore, sequence datasets and relative transcript expression levels were obtained using TPM values. Finally, an empirical DGE analysis was performed using the optimum parameters

(Ramakrishnan et al., 2022a). Genes with a false discovery rate (FDR)-corrected value of p cut-off of <0.05 and a fold change cut-off of \pm four-fold as a threshold value for being significant. Differentially expressed genes were functionally searched in a cloud BLAST using the CLC Genomic Workbench. Gene Ontology term identification was performed using three categories (biological processes, molecular functions, and cellular components), and similar names were identified from the Kyoto Encyclopedia of Genes and Genomes pathway database (Kanehisa, 2002; Kanehisa et al., 2017).

2.3.3 Quantitative-real time PCR analysis

To validate the RNA seq. Data, genes were selected for qRT-PCR based on their varied expression levels. Primers were designed using IDT primer design software (Supplementary Table 4). A synthesized cDNA template was used for qRT-PCR validation using SYBRTM Green PCR master mix (Applied Biosystems, United States) under the following parameters: 95°C for 3 min, 40 cycles of 95°C for 3 s, and 60°C for 34 s. A melting curve was generated to ensure single-product amplification and eliminate the possibility of primer dimers and nonspecific amplicons. The relative expression levels of the target genes were calculated using the $2^{-\Delta\Delta C_t}$ method with two housekeeping genes (Sellamuthu et al., 2022) as a reference for normalization with four biological replications.

2.4 Proteome

2.4.1 Sample preparation

Frozen beetles were dissected under on dry ice, and four biological replicates of each treatment were used for protein extraction and analysis. Each biological replicate contained tissue of three individual guts. Protein extraction was lysed in cold buffer containing 50 mM Tris-HCl, pH 7.5, 1 mM EDTA, 150 mM NaCl, 1% N-octylglycoside, and 0.1% sodium deoxycholate. Gut tissue in the buffer with protease inhibitor mixture (Roche) was incubated for 15 min on ice. Lysates were cleared by centrifugation, and after precipitation with chloroform/methanol, proteins were resuspended in 6 M urea, 2 M thiourea, 10 mM HEPES, pH 8.0 and proceeded for digestion (Cox et al., 2014).

2.4.2 Protein digestion

The samples were homogenized and lysed by boiling at 95°C for 10 min in 100 mM TEAB (triethylammonium bicarbonate) containing 2% SDC (sodium deoxycholate), 40 mM chloroacetamide, and 10 mM Tris (2-carboxyethyl) phosphine, and further sonicated (Bandelin Sonoplus Mini 20, MS 1.5). The protein concentration was determined using a standard protein assay kit (Thermo Fisher Scientific). About 30 μ g of protein per sample was used for MS sample preparation.

SP3 beads were used for sample processing. Five μ l of SP3 beads were mixed with 30 μ g protein in a lysis buffer and made up to 50 μ l with TEAB (100 mM). Protein binding was induced by adding ethanol to a final concentration of 60% (vol/vol). The samples were thoroughly mixed and incubated at 24°C for 5 min. After SP3 was bound to the proteins, the tubes were placed on a magnetic rack, and the remaining unbound supernatant was discarded. Using 180 μ l of 80% ethanol, beads were washed twice. After washing, samples were digested with trypsin (trypsin/protein ratio 1/30) and reconstituted in 100 mM TEAB at 37°C overnight. Digested samples were acidified with trifluoro acetic acid (TFA) to a final concentration of 1%. Finally,

peptides were desalted using in-house stage tips packed with C18 disks (Empore; Rappsilber et al., 2007).

2.4.3 Nanoliquid chromatography-MS/MS analysis

nLC-MS/MS analysis was performed with nano-reversed-phase columns (EASY-Spray column, 50 cm \times 75 μ m ID, PepMap C18, 2 μ m particles, 100 μ m pore size). In this analysis, mobile phase buffer A (0.1% formic acid in water) and mobile phase buffer B (acetonitrile and 0.1% formic acid) were used. Samples were loaded in a trap column of C18 PepMap100, 5 μ m particle size, 300 μ m \times 5 mm from Thermo Scientific. About 4 min at 18 μ l/min loading buffer with water, 2% acetonitrile, and 0.1% trifluoroacetic acid were used for loading. Peptides were eluted with a mobile phase B gradient of 4–35% over 120 min. The eluted peptide cations were converted into gas-phase ions by electrospray ionization. A Thermo Orbitrap Fusion (Q-OT-qIT, Thermo Scientific) was used for the analysis. Survey scans of peptide precursors from 350 to 1,400 m/z were performed using an Orbitrap at 120 K resolution (200 m/z) with a 5×10^5 ion count target. Tandem MS was isolated at 1.5 Th using a quadrupole, HCD fragmentation with a normalized collision energy of 30, and rapid scan analysis in the ion trap. The second mass spectral ion count target was set to 10^4 , and the maximum injection time was 35 ms. Precursors with charge state 2–6 were strictly sampled. The dynamic exclusion duration was set to 30 s with a 10 ppm tolerance around the selected precursor and its isotopes. Monoisotopic precursor selection was then performed. The instrument was run in top-speed mode with 2 s cycles (Hebert et al., 2014).

All data were analyzed and quantified using MaxQuant software (version 2.0.2.0; Cox and Mann, 2008). The FDR was limited to 1% for both full proteins and small peptides. The peptide lengths of the seven amino acids are specified. An MS/MS spectral search was performed using the Andromeda search engine against the *I. typographus* genome database. The C-termini of Arg and Lys were set for enzyme specificity, allowing the cleavage of proline bonds with a maximum of two missed cleavages. Cysteine dithiomethylation was selected as the fixed modification. Various modifications were considered with N-N-terminal protein acetylation and methionine oxidation. Matches between the run features from MaxQuant were used to transfer the identified peaks to other LC-MS/MS systems. Runs based on masses and retention times (with a maximum deviation of 0.7 min) were also considered for quantification. A label-free MaxQuant algorithm was used for quantification (Cox et al., 2014). Data analysis was performed using Perseus 1.6.15.0 (Tyanova et al., 2016).

2.5 Statistics

LC-MS data analysis was performed using MetaboAnalyst 4.0. GCxGC-TOF-MS data were cleaned for residual analysis, normalized (constant raw sum), and evaluated using principal component analysis (PCA) in the SIMCA 17 software (Sartorius Stedim Data Analytics AB, Malmö, Sweden). T-test with 95% confidence interval was used to compare the abundance of control and treatment groups in TIBCO Statistics (United States, 2021). The data from transcriptome and proteome was normalized using CLC workbench 21.0.5 (QIAGEN Aarhus, Denmark) and MaxQuant software (version 2.0.2.0) respectively, and significant data ($p < 0.05$) were extracted for further

analysis. qRT-data was analyzed with one-way ANOVA, Fisher LSD test in TIBCO Statistics (United States, 2021).

3 Results

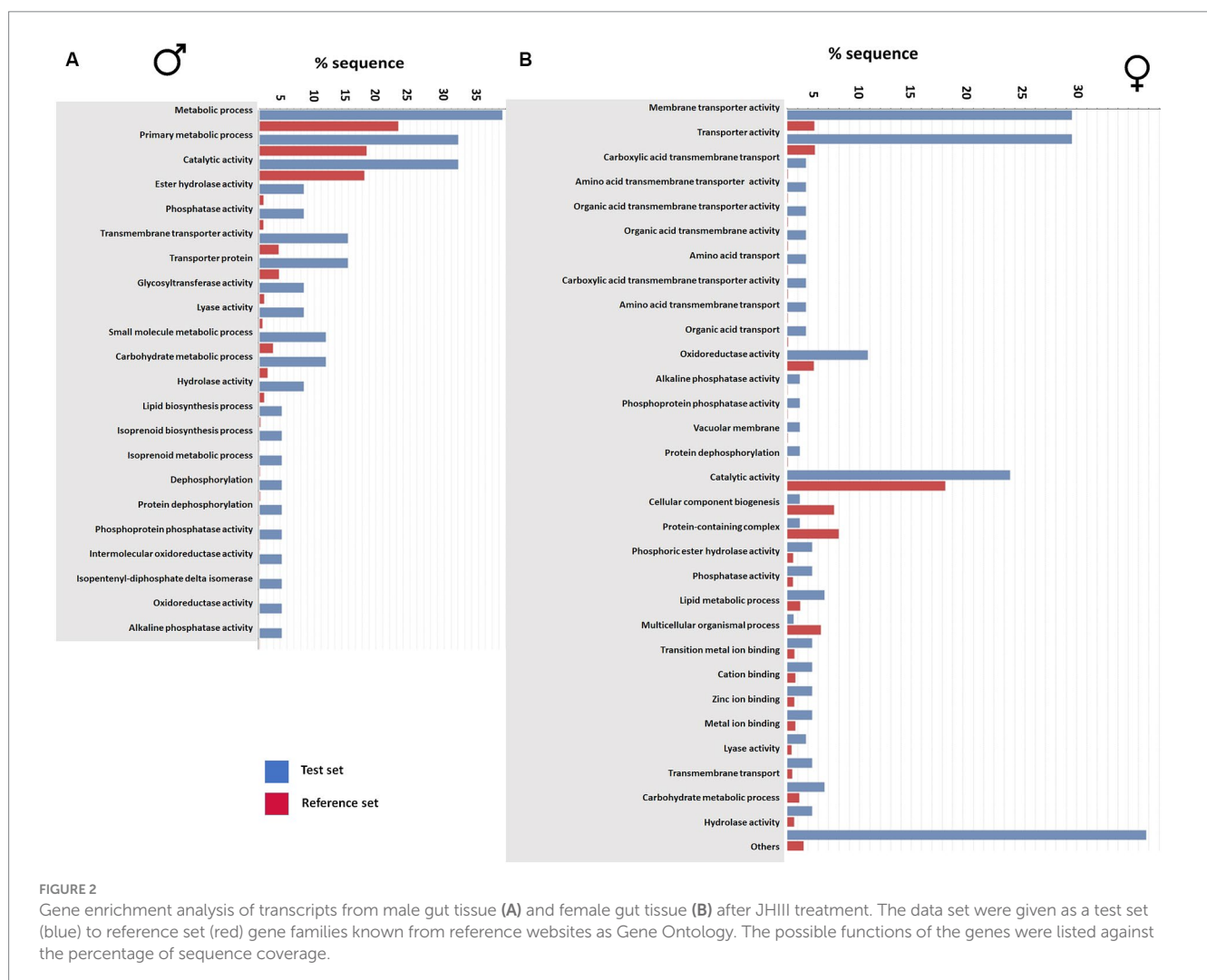
3.1 Total gene enrichment analysis from guts of males and females after JH III topical treatment

The functional aspects of JH III influenced gene families from adult males and females were gained by a gene enrichment analysis. The data gained from differential gene expression (DGE) with significance (FDR-corrected value of $p < 0.05$).

In males, the analysis revealed that a significant number of enriched genes were involved in metabolic processes. Additionally, functions such as catalytic activity, ester hydrolase, phosphatase activity, transporter and glycosyltransferase activities were also determined to be over-represented after JH III treatment by enrichment analysis. Gene functions related to lyase activity, small-molecule metabolic processes, carbohydrate metabolic processes, and

lipid biosynthesis were also over-represented. Most importantly, we found that gene groups involved in pheromone biosynthesis functions, including isoprenoid biosynthesis, metabolic processes, and dephosphorylation were enriched. Gene functions related to oxidoreductase and alkaline phosphatase activity had the least coverage in terms of gene sequences (Figure 2A).

In female gut tissue, the GEA showed enrichment of membrane-related and membrane transporter activity-related genes rather than metabolic synthesis genes as in males. Several gene groups with functions related to detoxification, such as carboxylic acid transmembrane transporter, organic acid membrane transporter, amino acid transporter, alkaline phosphate activity, phosphatase activity, and protein dephosphorylation were identified as enriched. Genes responsible for oxidoreductase and catalytic activities, phosphoric ester hydrolase activity, phosphatase, and lipid metabolism process had higher sequence coverage in females than males. Furthermore, metal ion binding genes such as zinc ion binding and, carbohydrate metabolic process gene families were identified exclusively in female gut tissue. The gene groups for lyase activity and hydrolase activity were enriched in females as in males and many unknown genes were clustered under the “others” category (Figure 2B). Taken together,



the gene enrichment analysis provided valuable insights into the over-representation of genes in males and females after JH III treatment.

3.2 Total protein enrichment analysis from guts of males and females after JH III topical treatment

The list of detected proteins was organized based on functional relevance. In the male gut tissue after JH III treatment, the identified proteins clustered into 456 known functions, while in the treated female gut formed 489 functional groups. Of these, 347 groups were common to both male-treated and female-treated gut samples. Similar to gene enrichment analysis, both sexes exhibited the highest numbers of plasma membrane-associated proteins (Supplementary Table 5).

The functional groups identified in male and female guts after JH III treatment were largely similar. Proteins related to the nucleus and nucleolus, ATP and RNA binding proteins were enriched in both sexes. However, in males, the number of proteins with functions related to metal ion binding and transferase activity was higher compared to females (Figure 3A). Whereas, in the female gut, the reproduction-related embryo development proteins were higher protein numbers (Figure 3B; Supplementary Table 5). Nevertheless, the differences between male and female guts after JH III treatment were minor in terms of gene transcripts and protein enrichments.

3.3 Metabolome

3.3.1 GC–MS analysis of extracts from guts and bodies of males and females after JH III topical treatment

Extracts of the guts and bodies of male and female *I. typographus* beetles subjected to JHIII treatment, were compared to their respective control groups, using comprehensive two-dimensional gas chromatography.

The initial Principal Component Analysis (PCA) revealed a distinct separation of JH III treated male gut samples from control samples treated with acetone. The first two components of the PCA plot accounted for 46.5% of the variance in the data (see Figure 4A). The primary compound responsible for this separation was identified as the main *I. typographus* aggregation pheromone component, 2-methyl-3-buten-2-ol. Additionally, compounds such as *cis*-verbenol and phenylethanol (male-specific compound) also contributed to this separation. In contrast, control male guts contained only phenylethanol and trace amounts of *cis*-verbenol, along with traces of other compounds such as verbenone, ipsdienol, and myrtenol (refer to Supplementary Figure 1).

The relative abundance of the pheromone precursor verbenyl oleate was determined in extracts from both the guts and the bodies (including the fat body) of beetles following JH III treatment and compared to a control (see Figure 4B). In both male and female beetle body extracts, JH III topical treatment led to a significant increase (1.5x in males, 15x in females) in the levels of verbenyl oleate compared to the control group.

This trend was also observed in extracts from female guts (15x increase). However, in the gut extracts of male beetles, JH III treatment resulted in a significant decrease (1.8x decrease) in the relative abundance of verbenyl oleate compared to the control group. This decrease is likely attributable cleavage of these monoterpene conjugates to give the free pheromone *cis*-verbenol (refer to Figure 4B). The absolute amount of verbenyl oleate in different beetle life stadia was 250 ng/mg of beetle body weight, as previously quantified (Ramakrishnan et al., 2022a) The content of free *cis*-verbenol in the guts of freshly emerged beetle was 5 ng/gut, which can be compared with control beetles in this study.

3.3.2 UHPLC-ESI-HRMS/MS analysis of guts extracts of males and females JH III topical treatment

Metabolic profiling of non-volatile and polar compounds in the gut tissues of JH III-treated males and females was conducted using a

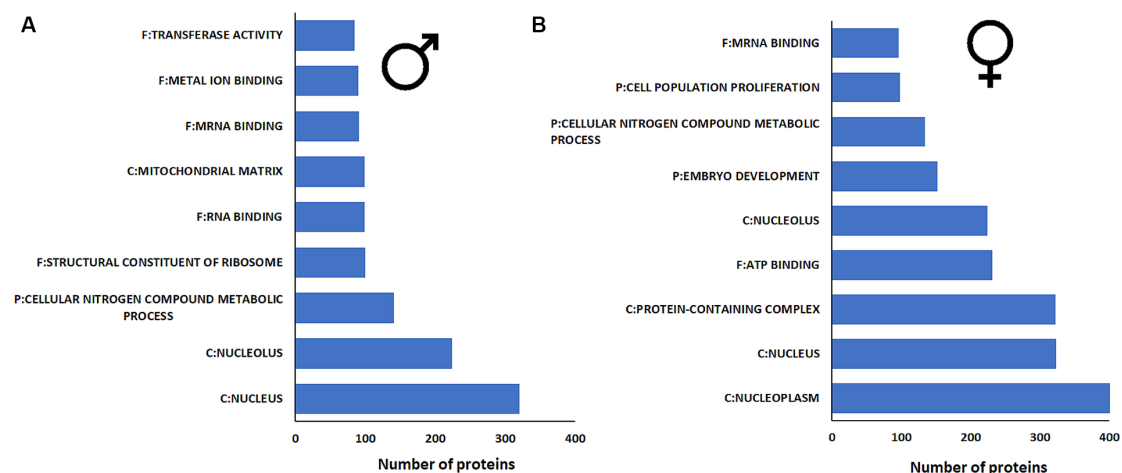
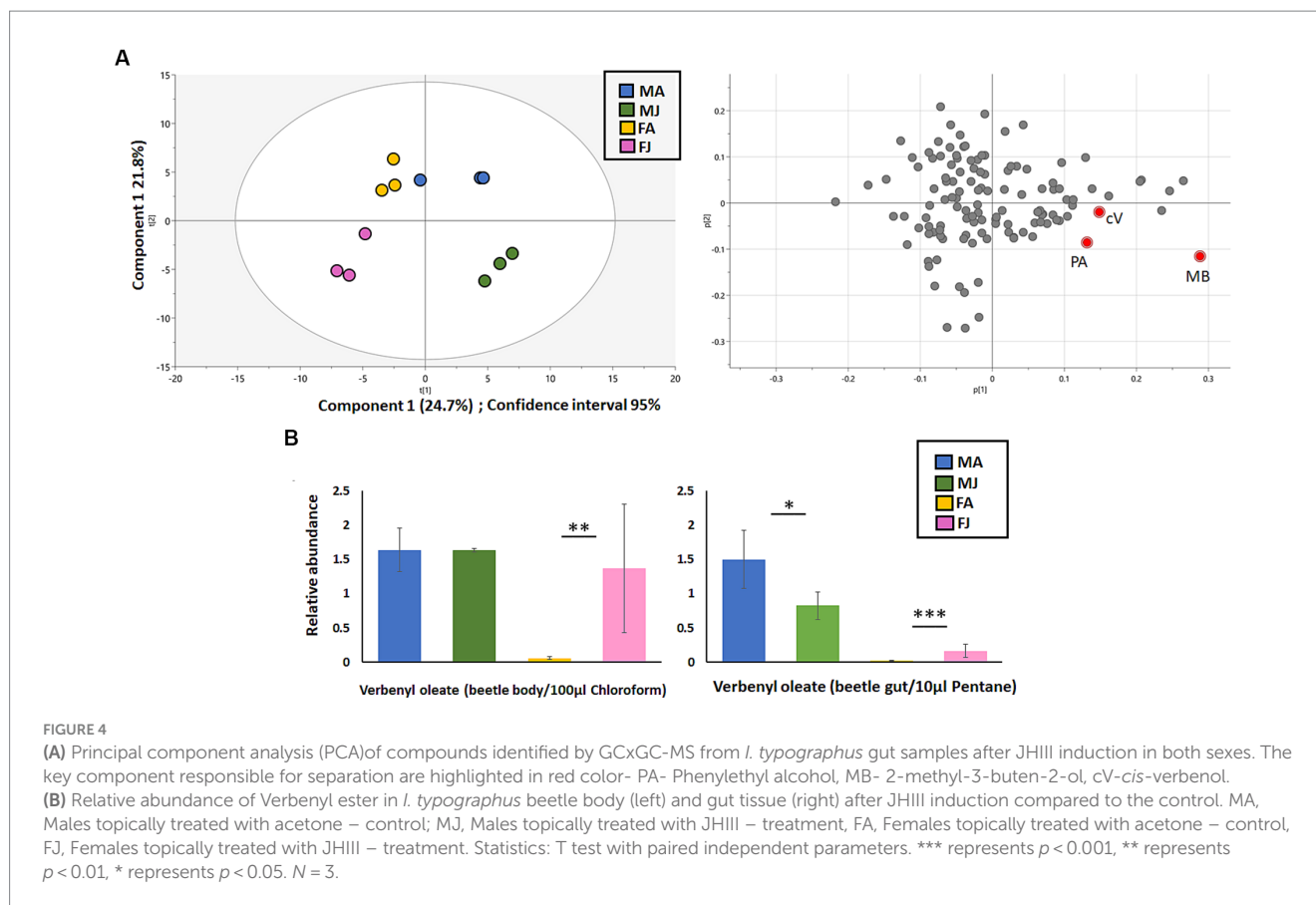


FIGURE 3

Protein enrichment analysis of proteins from (A) male gut tissue and (B) female gut tissue after JHIII treatment. The possible protein functions with significance $p < 0.05$ and functions containing more than 100 protein numbers are listed in this figure. A list of remaining functions with lower protein numbers are given in supplementary table 5.



non-targeted analysis via UHPLC/HRMS in both positive and negative ion modes. An unsupervised multivariate PCA was employed to assess differences among the sample groups.

In both ion modes measurements, JH III-treated males and females clustered distinct from the control group. In the negative ion mode, the PC analysis explained 55 and 61.2% of the total variance in males and females, respectively, (see Figure 5A, left). In the positive ion mode, the PC explained 60 and 50% of the total variance in males and females, respectively, (see Figure 5A, right). The determination of the total abundance of verbenyl diglycosides was calculated as the sum of the peak areas from the three individual verbenyl diglycoside peaks. After treatment with JH III in beetles, the total abundance of diglycosides content significantly increased in the guts of both sexes compared to the acetone-treated controls. There was no significant difference in the induction of these compounds by JH III between males and females (see Figure 5B). The actual amount of these compounds per beetle gut could not be determined due to the lack of standards.

3.4 Regulation of genes and proteins after JH III treatment in transcriptome and proteome of adult males and female beetles

3.4.1 Transcriptome-differential gene expression analysis

Overall, DGE analysis using the CLC workbench from the RNA sequence data obtained from beetle guts provided a clear distinction

between gene sets in JH III-treated versus control beetles and males versus females, with samples from each group clustered together in principal component analysis (Supplementary Figure 2A). After JH III treatment, approximately 710 transcripts were upregulated, and 545 were downregulated in male gut tissue only, as depicted in a Venn diagram (Figure 6A). On the other hand, in female gut tissue only a total of 518 transcripts were upregulated, and 456 transcripts were downregulated. However, approximately 5,155 transcripts were upregulated, and 4,595 transcripts were downregulated in both male and female gut tissues. Notably, the total number of genes upregulated after treatment in the male beetle gut was higher (10,385 transcripts) than that in the female beetles (9,682 transcripts; Figure 6A; Supplementary Table 1).

3.4.2 Proteome-differential protein expression analysis

The results of the DPE analysis of JH III-treated beetle gut tissue yielded a comprehensive list of identified proteins exhibiting a significant fold change in their expression following treatment. Samples from each treatment (JH III vs. control) were clustered in principal component analysis (Supplementary Figure 2B). It is noteworthy that although JH III treatment is conventionally associated with pheromone production in adult male beetles, the female beetle gut tissue exhibited a higher number of identified proteins after treatment, 449 versus 229 in males. Among the total number of upregulated proteins, 79 were male-specific, 302 were female specific and 145 were detected in both male and female guts. Among the total number of downregulated proteins, 68 proteins male specific, 69 were

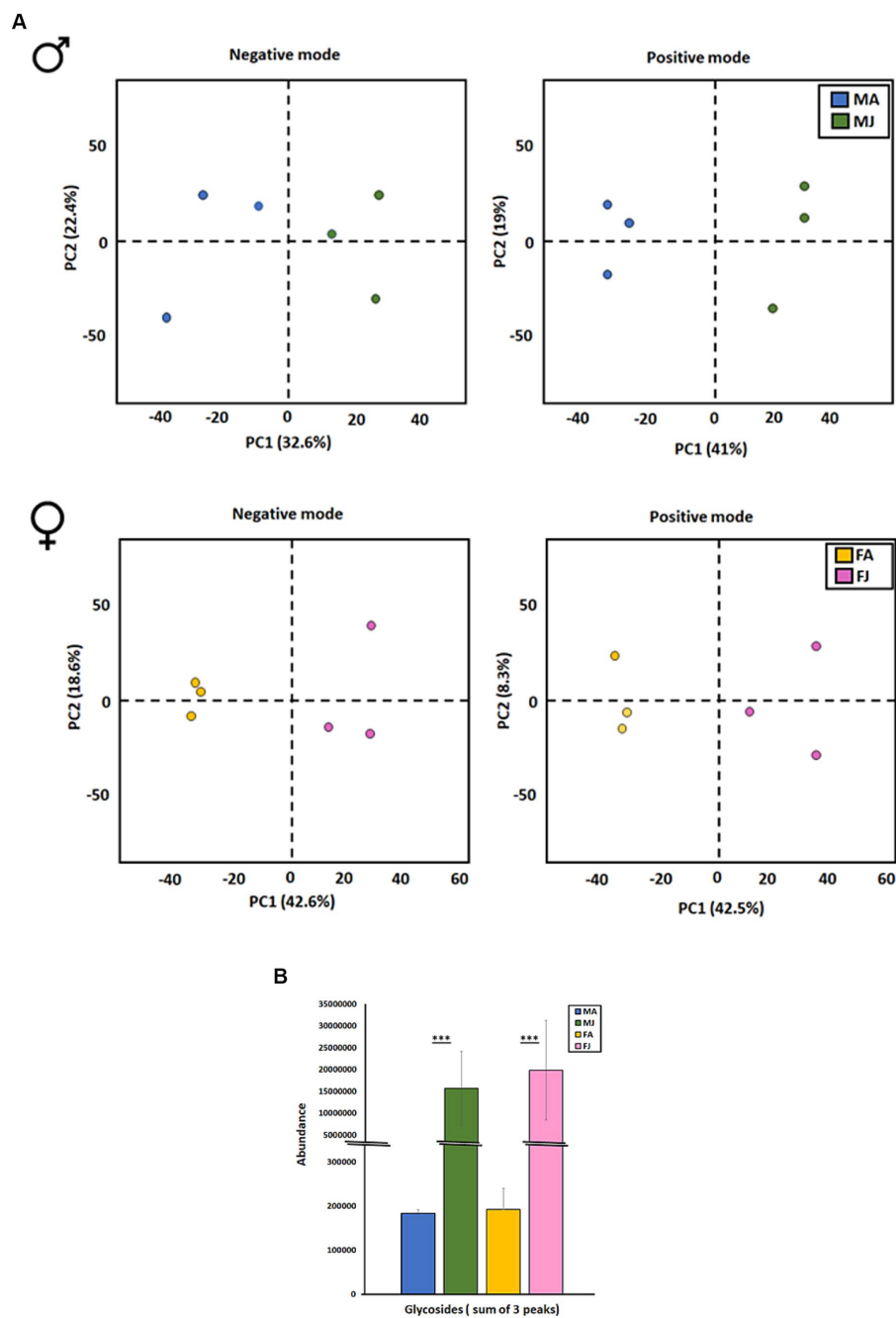


FIGURE 5
(A) Principal component analysis (PCA) of compounds identified by UHPLC-ESI-HRMS/MS analysis measured in negative (left) and positive mode (right). The data shows the overall separation of *I. typographus* gut samples after JHIII treatment in male (up) and female (down). **(B)** Abundance of Verbenyl di glycosides in *I. typographus* gut tissue after JHIII induction. MA, Males topically treated with acetone – control; MJ, Males topically treated with JHIII – treatment, FA, Females topically treated with acetone – control; FJ, Females topically treated with JHIII – treatment. T test with paired independent parameters. *** represents $p < 0.001$.

female specific and 27 were detected in both male and female guts (Figure 6B; Supplementary Table 2).

3.4.3 Comparison of transcriptome and proteome

To narrow down the upregulated genes from male gut tissue with possible functional significance, we compared the contig lists from the DGE and DPE analyses (Figure 6C). Although the number of identified proteins was 100-fold lower than the number of transcripts from the

DGE analysis, the results of the comparison helped identify a unique set of gene contigs for further evaluation. The male gut tissue had 129 contigs from transcript and protein analysis, names are provided in Supplementary Table 3A. The key mevalonate pathway gene Itp09271, isoprenyl-diphosphate synthase (IPDS) gene (functionally proposed for 2-methyl-3-buten-2-ol synthesis), was among the highly upregulated gene contigs. Other mevalonate pathway genes such as Itp06045 phosphomevalonate kinase (PMK), Itp09137,

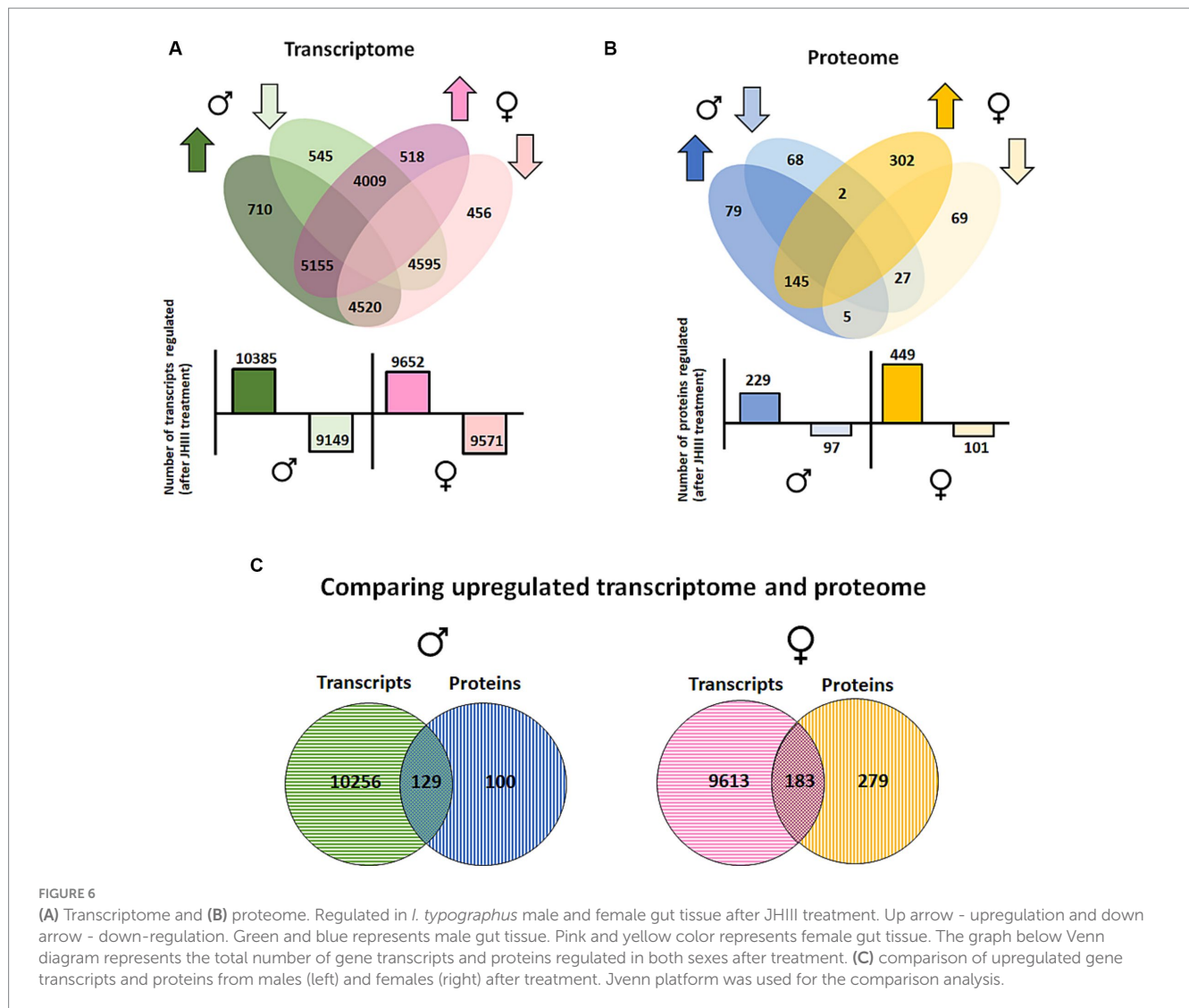


FIGURE 6

(A) Transcriptome and (B) proteome. Regulated in *I. typographus* male and female gut tissue after JHIII treatment. Up arrow - upregulation and down arrow - down-regulation. Green and blue represents male gut tissue. Pink and yellow color represents female gut tissue. The graph below Venn diagram represents the total number of gene transcripts and proteins regulated in both sexes after treatment. (C) comparison of upregulated gene transcripts and proteins from males (left) and females (right) after treatment. Jvenn platform was used for the comparison analysis.

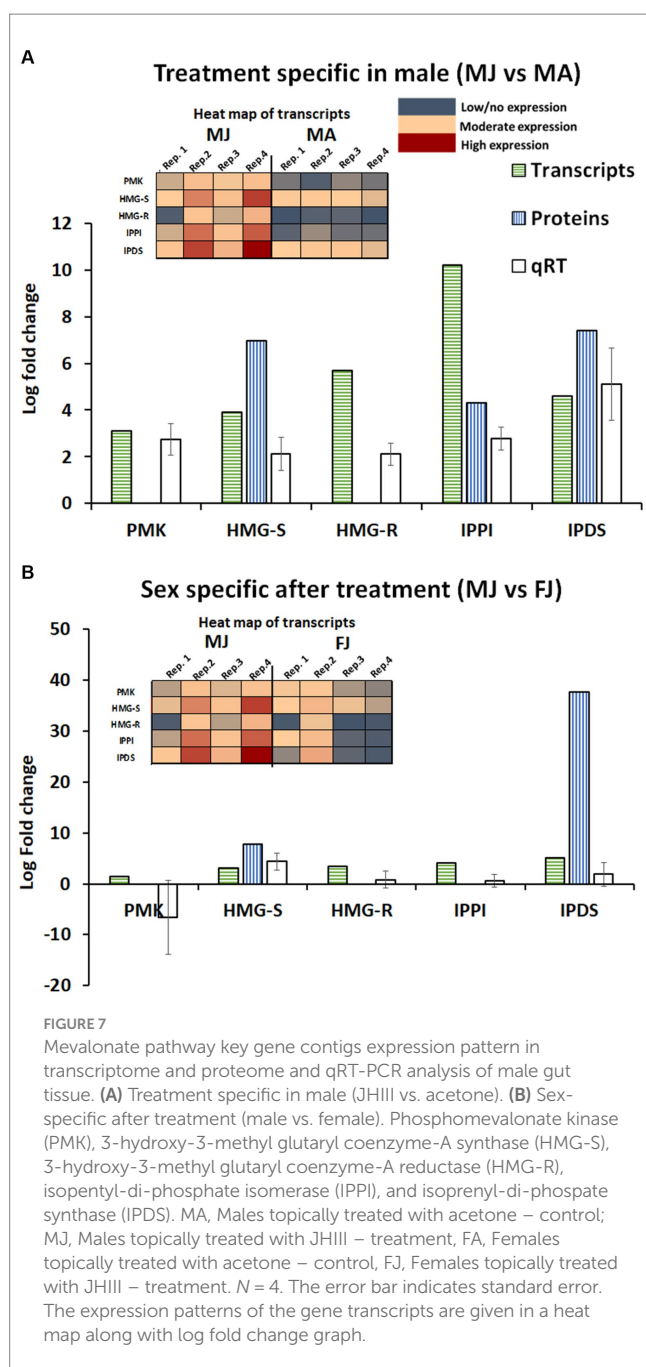
3-hydroxy-3methyl glutaryl Co-A synthase (HMG-S), and Ityp04875, isopentenyl-di-phosphate isomerase (IPPI) were also upregulated at the gene transcript level. A similar pattern was seen for the contigs involved in hydrolase function (listed in the table as myrosinase), which are known to have a functional role for glycosyl hydrolase activity, acting on glycosyl bonds (GO:0016798), and transferase contigs, such as acetyltransferase and UDP-glucuronosyltransferase (highlighted in Supplementary Table 3A). Many ribosomal and membrane transporter contigs, such as V-type ATPases, were also upregulated, while several genes that have an unknown function were identified among the male-specific upregulated gene contigs (Supplementary Table 3A).

The female gut tissue had approximately 183 contigs from transcripts and protein analysis (Figure 6C; Supplementary Table 3B). Although the number identified in females was higher than that in males, mevalonate pathway genes were not predominant in the list of identified contigs in females. However, another geranyl-diphosphate synthase (Ityp17861) was upregulated. Furthermore, gene families, such as glycine dehydrogenase, ubiquitin carboxyl-terminal hydrolase, and vitellogenin-like, with functions likely in detoxification and oocyte

formation, were found to be upregulated (Supplementary Table 3B). Similar to males, many genes related to mitochondria-related ribosomal proteins, elongation factors, binding proteins, and many functionally unknown genes and proteins were also found to be upregulated (Supplementary Table 3B).

3.4.4 Regulation of the mevalonate pathway after JH III treatment (involved in *de novo* pheromone biosynthesis)

Combining gene and protein expression with qRT-PCR allowed a more comprehensive overview of the effect of JHIII treatment and sex on the steps of the mevalonate pathway, which makes the *I. typographus* aggregation pheromones and pheromone precursors *de novo*. Information was obtained for the upregulation of the following genes by RNA-Seq and qRT-PCR: PMK (Ityp06045), HMG-S (Ityp09137), HMG-R (Ityp17150), IPPI (Ityp04875), and IPDS (Ityp09271; Figure 7A). Not all of these steps were identified at the protein level, but analysis revealed the upregulation of HMG-S, IPPI, and IPDS. Notably, we found that the IPDS gene was upregulated by up to 35-fold in male gut tissue compared with that in female gut tissue after JH III treatment (Figure 7B). Besides the IPDS gene,



HMG-S was also significantly upregulated in JH III treated male gut tissue compared with that in treated females (Figure 7B). Additionally, we also found that IPPI was exclusively abundant in proteins from female gut tissue after treatment (Supplementary Figure 3).

3.4.5 Regulation of the cytochromeP450 (CyP450) gene family after JH III treatment (involved in pheromone biosynthesis and pheromone formation from host tree precursors)

A similar combined approach was taken to explore the regulation of CyP450 genes that are involved in pheromone biosynthesis by RNA-Seq and qRT-PCR; no proteins of this family were detected in our proteomic investigation. CyP450 contigs showing expression patterns above a 2-fold change with a significant

value of p ($p < 0.05$) were confirmed by qRT-PCR analysis. Among the contigs previously proposed to be involved in pheromone biosynthesis (Ramakrishnan et al., 2022a), contigs Ityp3903 and Ityp0496 (proposed for verbenol synthesis), contigs Ityp3140 (proposed for detoxification), and Ityp3153 (proposed for ipsdienol) were all found to be upregulated genes in the JH III-treated male gut and are among the most highly upregulated genes measured in this study (Figure 8).

3.4.6 Regulation of esterase gene family after JH III treatment (involved in formation and cleavage of verbenyl fatty acid ester conjugates-possible pheromone precursors)

Among the esterase genes proposed for converting the stored verbenyl ester to *cis*-verbenol, Ityp11977 (which occurred in the early life stage) was not significantly influenced by JH III treatment in males according to transcriptome and proteome analysis. However, another esterase contig, Ityp09460, was found to be upregulated in the protein analysis and qRT-PCR but downregulated in the RNA-Seq transcriptome (Figure 9A). In female gut tissue, none of these contigs were detected, except for Ityp11977 in qRT-PCR (Figure 9B).

3.4.7 Regulation of Glycosyl hydrolase gene family after JH III treatment (involved in formation and cleavage of verbenyl diglycoside conjugates possible pheromone precursor)

When comparing DGE and DPE analyses in male gut tissue, a set of gene families known for glycosyl-hydrolase function (GO:0016798) was significantly upregulated after JHIII treatment at both the transcript and protein levels with male specificity. This gene family nearly as abundant as the genes of the mevalonate pathway, may cleave stored verbenyl glucoside conjugates to give the free pheromone. Twelve gene contigs were detected from the family, four of which were also detected and significantly upregulated at the protein level, Ityp11770, Ityp00535, Ityp00943, and Ityp04256. These were also upregulated by qRT-PCR except for contig Ityp11770 (Figure 10A). All three contigs were more upregulated in males than in females (Figure 10B); for females, DGE, DPE, and qRT-PCR did not show consistent upregulation after JHIII treatment (Figure 10B; Supplementary Figure 4).

4 Discussion

4.1 Changes in gene expression, proteins, and metabolites after JHIII application to *I. Typographus*, highlighting overall metabolic regulation

The topical application of JH III to adult beetles has been studied in many bark beetle species (Keeling et al., 2016; Tian et al., 2020). In *I. typographus*, we have identified numerous metabolic pathways affected by this hormone by changes in their genes, proteins, and metabolites. JH III treatment has been demonstrated to induce pheromone biosynthesis in male *I. typographus* exclusively and the formation of monoterpene detoxification conjugates in both sexes. These findings correlate with the earlier reported impact of JH III on other bark beetles such as *D. ponderosa* (Chiu et al., 2018).

JH III treatment led to the notable upregulation of metabolic processes and relevant membrane transporters, consistent with observations on other *Ips* species (Keeling et al., 2006). In addition, there were strong differences in gene expression patterns between males and females of *I. typographus* encompassing

functions such as catalytic activity, oxidoreductase activity, esterases, and phosphatases.

In male beetles, the treatment primarily influenced metabolic regulation, whereas, in females, it led to the induction of numerous reproduction-related genes such as vitellogenins (involved in oocyte biosynthesis). This observation can fit the well-documented influence of JH III on parenting behaviors in social insects (Trumbo, 2018). In addition to many membrane transporter activity genes in female guts, genes regulating detoxification processes, such as carboxylases and ubiquitin-carboxyl hydrolases were upregulated (Supplementary Table 3B).

A complementary protein enrichment analysis in this study also found sex-specific differences after JH III treatment. The male gut was enriched with proteins involved in metabolic processes and transferase activity-related proteins. These steps are key in the pheromone biosynthesis of *I. typographus* pioneer males. In the female gut after treatment, the embryo development-related proteins were among those upregulated (over 100 protein candidates), which correlated with the finding of vitellogenin upregulation at the gene level. Both sexes demonstrated upregulation of proteins involved in nuclear and detoxification processes. Unexpectedly, detoxification products of the host tree monoterpene-pinene, verbenyl fatty acid esters, were induced in the guts of both sexes by JHIII. This finding supports the recently proposed hypothesis that detoxification conjugates are produced in both sexes of bark beetles and later diverted to pheromone biosynthesis to the greatest extent in the pioneer sex in host finding-the males in *I. typographus* (Chiu et al., 2018; Ramakrishnan et al., 2022a). Nevertheless, the pathways involved in detoxification and pheromone biosynthesis need more study to understand the linkages between them.

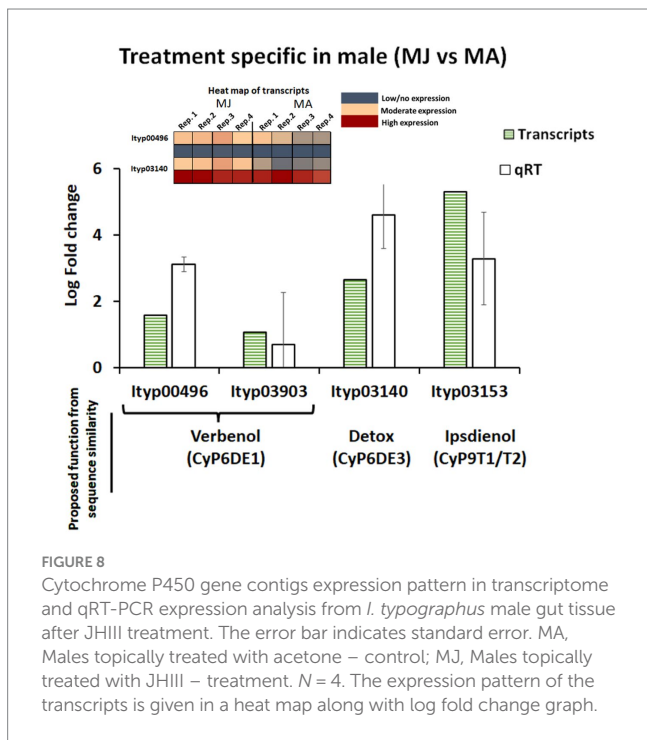


FIGURE 8 Cytochrome P450 gene contigs expression pattern in transcriptome and qRT-PCR expression analysis from *I. typographus* male gut tissue after JHIII treatment. The error bar indicates standard error. MA, Males typically treated with acetone – control; MJ, Males typically treated with JHIII – treatment. *N* = 4. The expression pattern of the transcripts is given in a heat map along with log fold change graph.

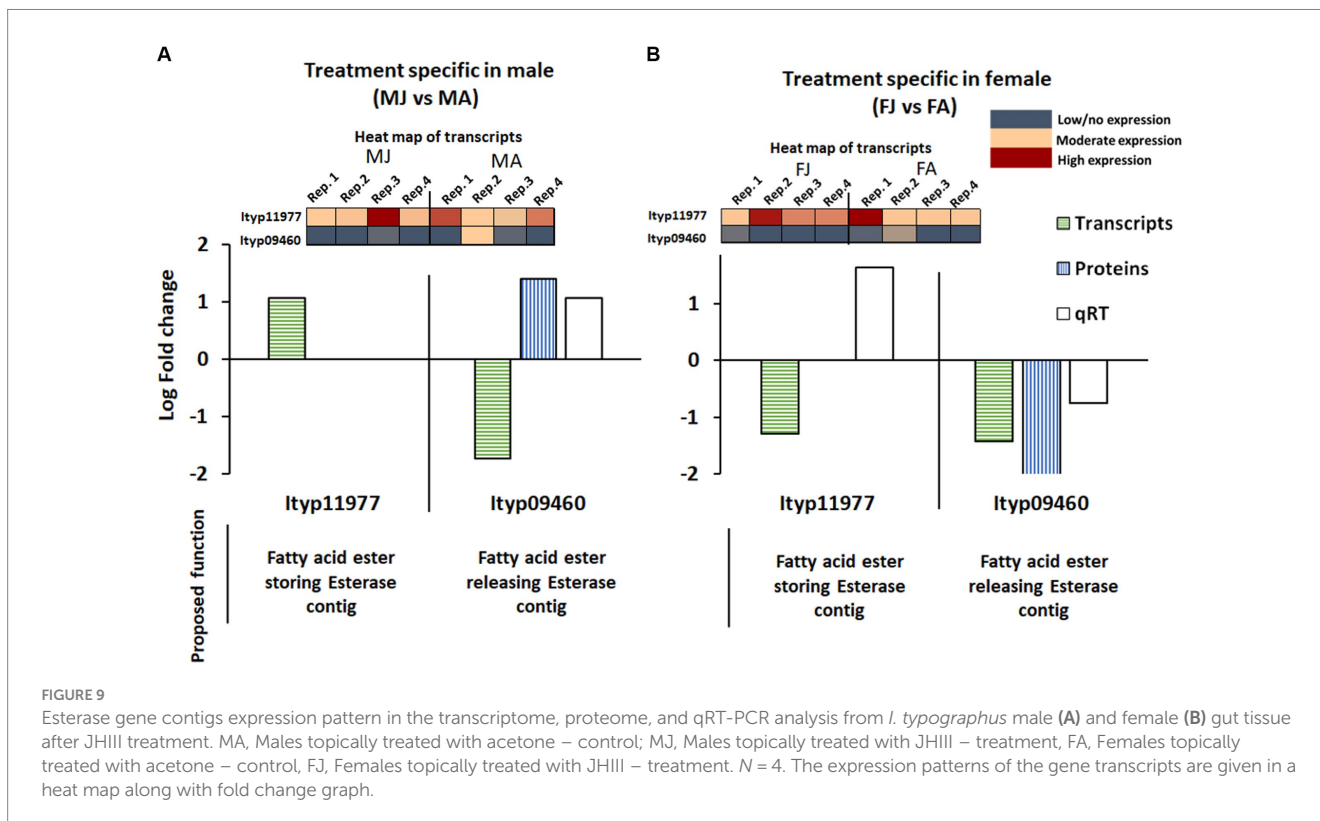


FIGURE 9 Esterase gene contigs expression pattern in the transcriptome, proteome, and qRT-PCR analysis from *I. typographus* male (A) and female (B) gut tissue after JHIII treatment. MA, Males typically treated with acetone – control; MJ, Males typically treated with JHIII – treatment, FA, Females typically treated with acetone – control, FJ, Females typically treated with JHIII – treatment. *N* = 4. The expression patterns of the gene transcripts are given in a heat map along with fold change graph.

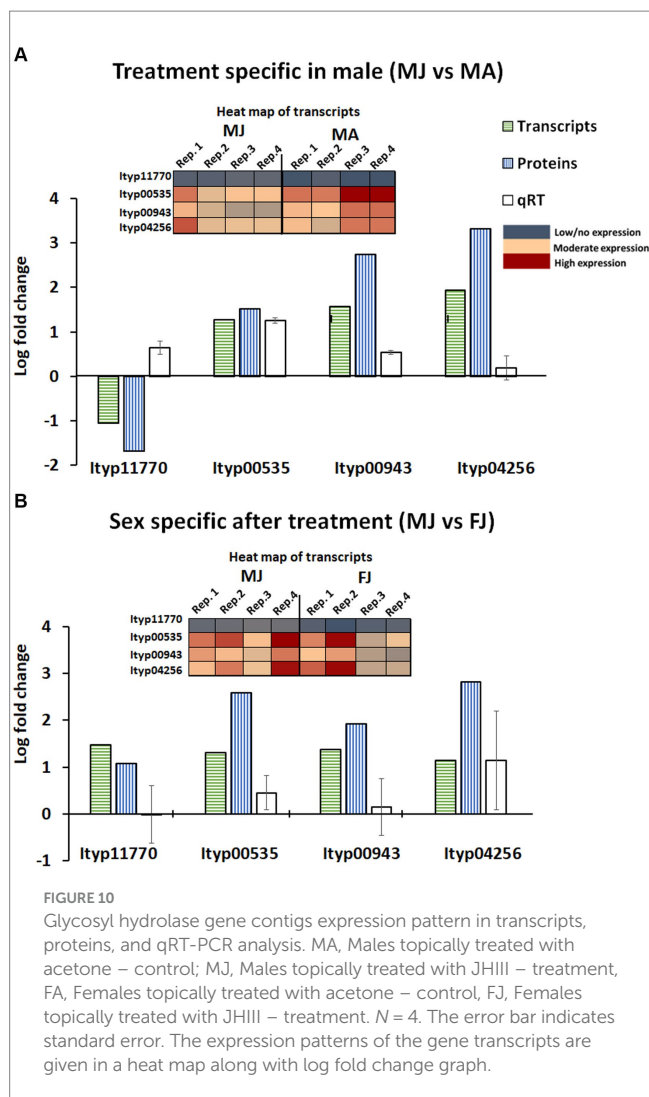


FIGURE 10
Glycosyl hydrolase gene contigs expression pattern in transcripts, proteins, and qRT-PCR analysis. MA, Males topically treated with acetone – control; MJ, Males topically treated with JHIII – treatment, FA, Females topically treated with acetone – control, FJ, Females topically treated with JHIII – treatment. $N = 4$. The error bar indicates standard error. The expression patterns of the gene transcripts are given in a heat map along with log fold change graph.

4.2 Identification of key genes responsible for pheromone biosynthesis

Two of the major male aggregation pheromone components of *I. typographus* are isoprenoids produced *de novo* by the mevalonate pathway were identified (Figure 7). The genes for this pathway have been annotated in the *I. typographus* genome (Powell et al., 2021; Naseer et al., 2023), and many of them are shown here to be upregulated exclusively in males. After JH III treatment, these genes have also been implicated in pheromone formation in other *Ips* species (Keeling et al., 2004).

In male *I. typographus*, topical treatment with JH III led to the overexpression of certain, upstream genes of the mevalonate pathway, including PMK (Ityp06045), HMG-S (Ityp09137), HMG-R (Ityp17150), and IPPI (Ityp04875). were relatively overexpressed in the gut. In addition, the upregulation of IPDS (Ityp09271) was observed at both the transcript and protein levels. This gene is a candidate for encoding the biosynthesis of the hemiterpene 2-methyl-3-buten-2-ol, which has not yet been functionally demonstrated. The upregulation of Ityp09271 aligns with the significant increase in 2-methyl-3-buten-2-ol content observed in the male gut after the treatment and corresponds with the biosynthetic pathway proposed

in our previous study (Ramakrishnan et al., 2022a). In females, there was also reported upregulation of another IPDS, an ortholog of geranyl diphosphate synthase (Ityp17861; Ivarsson et al., 1993).

In addition to the observed increase in the levels of 2-methyl-3-buten-2-ol induced by JH III, two other pheromone components were also upregulated: ipsdienol (presumably produced *de novo*) and *cis*-verbenol (likely synthesized from α -pinene) and sequestered as a fatty acid ester (Ramakrishnan et al., 2022a). GC-MS measurements of gut tissue following the induction further revealed a significant increase in *I. typographus* male-specific compounds, such as myrtenol and phenyl ethanol (Supplementary Figure 1). Although behavioral activity for these compounds has not been reported in *I. typographus*, they also produced by the pheromone-producing sex of related bark beetle species, *D. ponderosae* and *I. pini*, where their upregulation after the treatment has also been documented (Keeling et al., 2006, 2016). This suggests that the effect of JH III on pheromone biosynthesis is not limited solely to known behaviorally active compounds.

The effect of JH III- treatment on CyP450 enzymes was also studied, but this was only feasible at the gene transcript level as CyP450 proteins could not be identified in our proteomics work. In the transcriptome analysis, we searched for gene candidates with sequence similarities to functionally known genes from other bark beetle studies, including those involved in *cis*-verbenol biosynthesis (Chiu et al., 2019; Ramakrishnan et al., 2022a), detoxification mechanisms (CyP6DE3), and ipsdienol biosynthesis (CyP9T1/T2; Song et al., 2013; Nadeau et al., 2017).

Interestingly, CyP450s genes in all three functional classes were upregulated after JH III treatment with CyP6DE1, known in another bark beetle species for its role in *trans*-verbenol biosynthesis (Chiu et al., 2019). The contigs from *I. typographus* male gut exhibited lower expression levels compared to the gene contigs suggested for detoxification (CyP6DE3) and ipsdienol biosynthesis (CyP9T1/T2; Sandstrom et al., 2006). The effect of topically applied JH III on pheromone biosynthesis appears to be broader than just the induction of *de novo* synthesized compounds. In addition to regulating isoprenoid biosynthesis, this hormone affects the production of pheromonal components by influencing a variety of other biosynthetic mechanisms such as the hydroxylation of host tree monoterpenes.

4.3 Effects of JH III on the formation and cleavage of detoxification conjugates related to pheromonal components

In this study, topically applied JH III also influenced the production of verbenyl-fatty acid ester and verbenyl-diglycosides, which are conjugates of the pheromone *cis*-verbenol. Since *cis*-verbenol may also be regarded as a detoxification product of α -pinene, its esters, and glycosides may help to alleviate toxicity by stabilizing the initial detoxification product. However, our main objective was to test the hypothesis that these esters and glycosides are precursors of *cis*-verbenol in adult males when they need to release large quantities of these pheromones during the attack on the host tree.

Furthermore, the compound, verbenyl-oleate production after JH III treatment has significantly induced in the fat bodies of both sexes of adult beetles. The induction rate was 10 times higher in females than in males. We previously established from the production curve of this compound at different life stages (Ramakrishnan et al., 2022a) that verbenyl oleate

abundance is male-specific during adult beetle stages. However, in this study, we report that treatment can also induce its production in female adult beetles. This finding suggests a strong regulatory role for JH III in the formation of these compounds in the beetle.

The content of verbenyl oleate in the gut is 100 times lower than in the fat body of *I. typographus* (Ramakrishnan et al., 2022a). Despite the gut being the site for biosynthesis of this compound during the juvenile stages and later in adult males free *cis*-verbenol release occurs. Also, JH III induced an increase in verbenyl oleate abundance in female guts similar to that in the fat body and reduced its content in male guts. These findings support the existing hypothesis that the cleavage of verbenyl fatty acyl esters is specific to adult males and that verbenyl esters serve as precursors for the active pheromonal *cis*-verbenol in pioneer male *I. typographus* (Ramakrishnan et al., 2022a). Both the formation and cleavage steps of verbenyl fatty acid esters are regulated by JH III, indicating that the responsible enzymes (esterase, also known as carboxylesterases or fatty acid transferases) are likely regulated at the gene or protein level.

The esterase contig Ityp11977, which was previously reported in earlier life stages of *I. typographus* for verbenyl fatty acyl ester formation (Ramakrishnan et al., 2022a), was also identified in the guts of beetles after treatment. This observation aligns with the finding that the candidate Ityp11977 was exclusively expressed (as shown in qRT-PCR analysis) in the female gut after treatment (see Figure 9). We also identified another contig from esterase - Ityp09460, expressed in the male gut following the treatment, coinciding with a reduction in verbenyl ester levels. This observation leads us to propose the involvement of this esterase candidate in the release of *cis*-verbenol through the cleavage of ester bonds in the male gut, a novel finding in *I. typographus*. It is worth noting that this esterase is known for several detoxification functions in other insects (Blomquist et al., 2021).

In our previous study, other *cis*-verbenyl conjugates in the guts of beetles were identified as three verbenyl-diglycosides differing structurally by glycosidic parts (Ramakrishnan et al., 2022a,b). Glycosylated alcohols are known to serve as detoxification products, and they may have relevance to bark beetle pheromone biosynthesis in other species (Blomquist et al., 2021). In this study, we observed a significant 100-fold increase in the content of these compounds in the guts following the treatment, and this induction showed similar rates in both sexes of adult beetles. This demonstrates the JH III regulation over the formation of these compounds.

Furthermore, to test the hypothesis that these compounds could serve as alternative pheromonal *cis*-verbenol precursors, we searched and identified for possible genes within specific glycosyl hydrolase gene families. Later, the gene for potential male-specific release to free *cis*-verbenol. Notably, we identified four contigs from the glycosyl hydrolase gene family that were overexpressed exclusively in the male gut after treatment. However, the uncertainty in the abundance of male-specific verbenyl diglycosides (not similar to verbenyl ester), together with low quantity in the gut and absence in the fat body (unpublished data) we presume that these compounds are more likely a detoxification product rather than a pheromone precursor. Thus, we have observed a strong induction of JH III on the formation of both verbenyl conjugates discussed. Originally, these compounds serve as binding agents for the detoxification product of α -pinene, specifically *cis*-verbenol in our case, but additionally, our findings proved that verbenyl fatty acyl esters are possessed by adult males as an alternative pheromone precursor (Chiu et al., 2018; Ramakrishnan et al., 2022a).

Hence, obtaining the specific gene candidates directs us to practical application by targeting the genes of pheromone biosynthesis for silencing in *I. typographus*. Targeting the species-specific non-lethal genes of the beetle along with characterizing them aims to address the pest's aggregation behavior with minimum ecological damage. A similar approach was demonstrated in a moth, *Helicoverpa armigera* when reproduction was modified by silencing genes responsible for sex pheromones production (Dong et al., 2017).

The main objective of RNAi-based Forest pest management is to reduce the forest pest population level below the epidemic level (Hlasny et al., 2021). Similarly, genes involved in pheromone production in bark beetles can be targeted via RNAi to disrupt communication, such as aggregation of pheromone signal for a mass attack in *I. typographus*. However, selecting an appropriate delivery method for specific insect orders is challenging. In wood-feeding insects, the aspect of dsRNA delivery can be achieved by spraying over the tree trunk (Li et al., 2015) or by injecting it into the tree's sap stream (Hunter et al., 2012). The delivery of dsRNA by these methods will be used for effective silencing of the pheromone biosynthetic genes in the beetle upon phloem-feeding. However, appropriate method should be considered while choosing the for effective outcome (Joga et al., 2021). This approach is familiar with existing forest pest management practices (i.e., silvicultural, biological), and can aid a multi-faceted management approach that keeps the tree-killing forest pest populations in the endemic stage while conserving the beneficial species.

In conclusion, these findings establish a foundation for understanding the genetic mechanisms underlying pheromone biosynthesis in *I. typographus* following JH III treatment. However, a logical next step would be to conduct functional validation of the identified gene candidates involved in pheromone biosynthesis. This approach could lead to effective pest management strategies, such as RNA interference, aimed at manipulating the mass attack behavior of this aggressive pest (Joga et al., 2021).

Data availability statement

All the data and resources generated for this study are included in the article and the supplemental materials. The RNA sequences have been submitted in NIH under the accession PRJNA934749. The Proteome data have been submitted in Proteome Xchange under the identifier PXD039243. We are willing to share all the data and resources in this study with the public.

Ethics statement

Ethical approval was not required for the study involving animals in accordance with the local legislation and institutional requirements because We have performed all beetle experiments that comply with the ARRIVE guidelines and were carried out in accordance with (Scientific Procedures) Act, 1986 and associated guidelines, EU Directive 2010/63/EU for animal experiments.

Author contributions

RR: conceptualization, methodology, formal analysis, resources, and writing – original draft. AR: RNA-seq, data curation, molecular

work support, and writing – review and editing. JH: GC-metabolomic data analysis and method writing. MK: UHPLC/HRMS-MS data analysis. KH: proteomics data analysis and method writing. AS: UHPLC/HRMS-MS data analysis and reviewing. AJ: conceptualization, methodology, formal analysis, writing – review and editing, and supervision. All authors contributed to the article and approved the submitted version.

Funding

RR, AR, JH, AS, and AJ are supported by Czech Science Foundation “GACR,” no. 23-07916S; RR was supported by IGA A_20_22 RAJARAJAN RAMAKRISHNAN at the Faculty of Forestry and Wood Sciences, Czech University of Life sciences, Prague, CR; AR is supported by Excellent team grant 202 3–24, Faculty of Forestry and Wood Sciences, Czech University of Life Sciences, Prague, CR; AR, JH, and AJ were supported by Ministry of Education, Youth and Sport, Operational Program Research, Development and Education “EXTEMIT-K,” no. CZ.02.1.01/0.0/0.0/15_003/0000433.

Acknowledgments

We acknowledge the editing and valuable comments of Jonathan Gershenson on the final manuscript version and the constructive

References

- Bakke, A., Froyen, P., and Skattebol, L. (1977). Field response to a new pheromonal compound isolated from *Ips typographus*. *Naturwissenschaften* 64, 98–99. doi: 10.1007/bf00437364
- Bearfield, J. C., Henry, A. G., Tittiger, C., Blomquist, G. J., and Ginzler, M. D. (2009). Two regulatory mechanisms of Monoterpenoid pheromone production in *Ips* spp. of bark beetles. *J. Chem. Ecol.* 35, 689–697. doi: 10.1007/s10886-009-9652-2
- Blomquist, G. J., Figueroa-Teran, R., Aw, M., Song, M. M., Gorzalski, A., Abbott, N. L., et al. (2010). Pheromone production in bark beetles. *Insect Biochem. Mol. Biol.* 40, 699–712. doi: 10.1016/j.ibmb.2010.07.013
- Blomquist, G. J., Tittiger, C., MacLean, M., and Keeling, C. I. (2021). Cytochromes P450: terpene detoxification and pheromone production in bark beetles. *Current Opinion in Insect Sci.* 43, 97–102. doi: 10.1016/j.cois.2020.11.010
- Buhaescu, I., and Izzedine, H. (2007). Mevalonate pathway: a review of clinical and therapeutical implications. *Clin. Biochem.* 40, 575–584. doi: 10.1016/j.clinbiochem.2007.03.016
- Byers, J. A., and Birgersson, G. (1990). Pheromone production in a bark beetle independent of myrcene precursor in host pine species. *Naturwissenschaften* 77, 385–387. doi: 10.1007/bf01135739
- Chiu, C. C., Keeling, C. I., and Bohlmann, J. (2018). Monoterpenyl esters in juvenile mountain pine beetle and sex-specific release of the aggregation pheromone *trans-verbenol*. *Proc. Natl. Acad. Sci. U. S. A.* 115, 3652–3657. doi: 10.1073/pnas.1722380115
- Chiu, C. C., Keeling, C. I., and Bohlmann, J. (2019). The cytochrome P450 CYP6DE1 catalyzes the conversion of α -pinene into the mountain pine beetle aggregation pheromone *trans-verbenol*. *Sci. Rep.* 9:1477. doi: 10.1038/s41598-018-38047-8
- Chong, J., Soufan, O., Li, C., Caraus, I., Li, S. Z., Bourque, G., et al. (2018). MetaboAnalyst 4.0: towards more transparent and integrative metabolomics analysis. *Nucleic Acids Res.* 46, W486–W494. doi: 10.1093/nar/gky310
- Cox, J., Hein, M. Y., Lubner, C. A., Paron, I., Nagaraj, N., and Mann, M. (2014). Accurate proteome-wide label-free quantification by delayed normalization and maximal peptide ratio extraction. *Termed MaxLFQ. Molecular & Cellular Proteomics* 13, 2513–2526. doi: 10.1074/mcp.M113.031591
- Cox, J., and Mann, M. (2008). MaxQuant enables high peptide identification rates, individualized p.p.b.-range mass accuracies and proteome-wide protein quantification. *Nat. Biotechnol.* 26, 1367–1372. doi: 10.1038/nbt.1511
- Cristino, A. S., Nunes, F. M., Lobo, C. H., Bitondi, M. M., Simões, Z. L., da Fontoura Costa, L., et al. (2006). Caste development and reproduction: a genome-wide analysis of hallmarks of insect eusociality. *Insect Mol. Biol.* 15, 703–714. doi: 10.1111/j.1365-2583.2006.00696.x

comments of Fredrik Schlyter, Hynek Burda and Ewald Grosse-Wilde on the earlier version of the manuscript.

Conflict of interest

The authors declare that the research was conducted in the absence of any commercial or financial relationships that could be construed as a potential conflict of interest.

Publisher's note

All claims expressed in this article are solely those of the authors and do not necessarily represent those of their affiliated organizations, or those of the publisher, the editors and the reviewers. Any product that may be evaluated in this article, or claim that may be made by its manufacturer, is not guaranteed or endorsed by the publisher.

Supplementary material

The Supplementary material for this article can be found online at: <https://www.frontiersin.org/articles/10.3389/ffgc.2023.1215813/full#supplementary-material>

- Dai, L. L., Gao, H. M., and Chen, H. (2021). Expression levels of detoxification enzyme genes from *Dendroctonus armandi* (Coleoptera: Curculionidae) fed on a solid diet containing pine phloem and Terpenoids. *Insects* 12:15. doi: 10.3390/insects12100926
- Dhandapani, R. K., Gurusamy, D., Duan, J. J., and Palli, S. R. (2020). RNAi for management of Asian long-horned beetle, *Anoplophora glabripennis*: identification of target genes. *J. Pest Sci* 93, 823–832. doi: 10.1007/s10340-020-01197-8
- Dong, K., Sun, L., Liu, J. T., Gu, S. H., Zhou, J.-J., Yang, R.-N., et al. (2017). RNAi-Induced Electrophysiological and Behavioral Changes Reveal Two Pheromone Binding Proteins of *Helicoverpa armigera* Involved in the Perception of the Main Sex Pheromone Component Z11-16:Ald. *J. Chem. Ecol.* 43, 207–214. doi: 10.1007/s10886-016-0816-6
- Emlen, D., Szafran, Q., Corley, L., and Dworkin, I. (2006). Insulin signaling and limb-patterning: candidate pathways for the origin and evolutionary diversification of beetle 'horns'. *Heredity* 97, 179–191. doi: 10.1038/sj.hdy.6800868
- Fang, J. X., Zhang, S. F., Liu, F., Cheng, B., Zhang, Z., Zhang, Q. H., et al. (2021a). Functional investigation of monoterpenes for improved understanding of the relationship between hosts and bark beetles. *J. Appl. Entomol.* 145, 303–311. doi: 10.1111/jen.12850
- Fang, J. X., Du, H. C., Shi, X., Zhang, S. F., Liu, F., Zhang, Z., et al. (2021b). Monoterpenoid signals and their transcriptional responses to feeding and juvenile hormone regulation in bark beetle *Ips hauseri*. *J. Exp. Biol.* 224:9. doi: 10.1242/jeb.238030
- Gilg, A. B., Bearfield, J. C., Tittiger, C., Welch, W. H., and Blomquist, G. J. (2005). Isolation and functional expression of an animal geranyl diphosphate synthase and its role in bark beetle pheromone biosynthesis. *Proc. Natl. Acad. Sci. U. S. A.* 102, 9760–9765. doi: 10.1073/pnas.0503277102
- Goodman, W. G., and Cusson, M. (2012). The juvenile hormones. *Insect Endocrinol.* 8, 310–365. doi: 10.1016/B978-0-12-384749-2.10008-1
- Hebert, A. S., Richards, A. L., Bailey, D. J., Ulbrich, A., Coughlin, E. E., Westphal, M. S., et al. (2014). The one hour yeast proteome. *Mol. Cell. Proteomics* 13, 339–347. doi: 10.1074/mcp.M113.034769
- Hilliou, F., Chertemps, T., Maibeche, M., and Le Goff, G. (2021). Resistance in the genus *Spodoptera*: key insect detoxification genes. *Insects* 12:27. doi: 10.3390/insects12060544
- Hlasny, T., König, L., Krokene, P., Lindner, M., Montagne-Huck, C., Müller, J., et al. (2021). Bark beetle outbreaks in Europe: state of knowledge and ways forward for management. *Current Forestry Reports* 7, 138–165. doi: 10.1007/s40725-021-00142-x
- Hughes, P. R. (1974). Myrcene - precursor of pheromones in *Ips* beetles. *J. Insect Physiol.* 20, 1271–1275. doi: 10.1016/0022-1910(74)90232-7

- Hunter, W. B., Glick, E., Paldi, N., and Bextine, B. R. (2012). Advances in RNA interference: dsRNA Treatment in Trees and Grapevines for Insect Pest Suppression. *Southwest. Entomol.* 37, 85–87. doi: 10.3958/059.037.0110
- Ivarsson, P., and Birgersson, G. (1995). Regulation and biosynthesis of pheromone components in the double spined bark beetle *Ips duplicatus* (Coleoptera, Scolytidae). *J. Insect Physiol.* 41, 843–849. doi: 10.1016/0022-1910(95)00052-v
- Ivarsson, P., Schlyter, F., and Birgersson, G. (1993). Demonstration of *de-novo* pheromone biosynthesis in *Ips duplicatus* (Coleoptera, Scolytidae) - inhibition of ipsdienol and e-myrcenol production by compactin. *Insect Biochem. Mol. Biol.* 23, 655–662. doi: 10.1016/0965-1748(93)90039-u
- Jindra, M., and Bittova, L. (2020). The juvenile hormone receptor as a target of juvenoid "insect growth regulators". *Arch. Insect Biochem. Physiol.* 103:e21615. doi: 10.1002/arch.21615
- Jindra, M., Palli, S. R., and Riddiford, L. M. (2013). "The juvenile hormone signaling pathway in insect development" in *Annual review of entomology*. ed. M. R. Berenbaum, vol. 58, 181–204. doi: 10.1146/annurev-ento-120811-153700
- Joga, M. R., Moglicherla, K., Smaghe, G., and Roy, A. (2021). RNA interference-based forest protection products (FPPs) against wood-boring coleopterans: Hope or hype? *Front. Plant Sci.* 12:733608. doi: 10.3389/fpls.2021.733608
- Kanehisa, M. (2002). The KEGG database. *Silico Simulation of Biolog. Processes* 247, 91–103. doi: 10.1002/0470857897.ch8
- Kanehisa, M., Furumichi, M., Tanabe, M., Sato, Y., and Morishima, K. (2017). KEGG: new perspectives on genomes, pathways, diseases and drugs. *Nucleic Acids Res.* 45, D353–D361. doi: 10.1093/nar/gkw1092
- Keeling, C. I., Bearfield, J. C., Young, S., Blomquist, G. J., and Tittiger, C. (2006). Effects of juvenile hormone on gene expression in the pheromone-producing midgut of the pine engraver beetle, *Ips pini*. *Insect Mol. Biol.* 15, 207–216. doi: 10.1111/j.1365-2583.2006.00629.x
- Keeling, C. I., Blomquist, G. J., and Tittiger, C. (2004). Coordinated gene expression for pheromone biosynthesis in the pine engraver beetle, *Ips pini* (Coleoptera: Scolytidae). *Naturwissenschaften* 91, 324–328. doi: 10.1007/s00114-004-0523-y
- Keeling, C. I., Li, M., Sandhu, H. K., Henderson, H., Saint Yuen, M. M., and Bohlmann, J. (2016). Quantitative metabolome, proteome and transcriptome analysis of midgut and fat body tissues in the mountain pine beetle, *Dendroctonus ponderosae* Hopkins, and insights into pheromone biosynthesis. *Insect Biochem. Mol. Biol.* 70, 170–183. doi: 10.1016/j.ibmb.2016.01.002
- Knizek, M., Zahradnik, P., and Liška, J. (2023). Sborník referátů z celostátního semináře s mezinárodní účastí Přípravky na ochranu lesa – realita a budoucnost. *Zpravodaj ochrany lesa, Škodliví činitelé v lesích Česka. Svazek.* 26, 2022/23.
- Kyre, B. R., Bentz, B. J., and Rieske, L. K. (2020). Susceptibility of mountain pine beetle (*Dendroctonus ponderosae* Hopkins) to gene silencing through RNAi provides potential as a novel management tool. *For. Ecol. Manag.* 73, 0378–1127. doi: 10.1016/j.foreco.2020.118322
- Leinwand, S. G., and Scott, K. (2021). Juvenile hormone drives the maturation of spontaneous mushroom body neural activity and learned behavior. *Neuron* 109, 1836–1847.e5. doi: 10.1016/j.neuron.2021.04.006
- Li, H., Guan, R., Guo, H., and Miao, X. (2015). New insights into an RNAi approach for plant defence against piercing-sucking and stem-borer insect pests. *Plant Cell Environ.* 38:2277–2285. doi: 10.1111/pce.12546
- Nadeau, J. A., Petereit, J., Tillett, R. L., Jung, K., Fotoohi, M., MacLean, M., et al. (2017). Comparative transcriptomics of mountain pine beetle pheromone-biosynthetic tissues and functional analysis of CYP6DE3. *BMC Genomics* 18:311. doi: 10.1186/s12864-017-3696-4
- Nardi, J. B., Young, A. G., Ujhelyi, E., Tittiger, C., Lehane, M. J., and Blomquist, G. J. (2002). Specialization of midgut cells for synthesis of male isoprenoid pheromone components in two scolytid beetles, *Dendroctonus jeffreyi* and *Ips pini*. *Tissue Cell* 34, 221–231. doi: 10.1016/s0040-8166(02)00004-6
- Naseer, A., Moglicherla, K., Sellamuthu, G., and Roy, A. (2023). Age matters life-stage, tissue, and sex-specific gene expression dynamics in *Ips typographus* (Coleoptera: Curculionidae: Scolytinae). *Front. for. glob.* 6:1124754. doi: 10.3389/ffgc.2023.1124754
- NIST (2017). Inorganic Crystal Structure Database. *NIST Standard Reference Database Number 3*. Gaithersburg MD: National Institute of Standards and Technology. 20899. doi: 10.18434/M32147
- Pandey, A., and Bloch, G. (2015). Juvenile hormone and ecdysteroids as major regulators of brain and behavior in bees. *Current Opinion in Insect Sci.* 12, 26–37. doi: 10.1016/j.cois.2015.09.006
- Patacca, M., Lindner, M., Lucas-Borja, M. E., Cordonnier, T., Fidej, G., Gardiner, B., et al. (2023). ISignificant increase in natural disturbance impacts on European forests since 1950. *Glob. Change Biol.* 29, 1359–1376. doi: 10.1111/gcb.16531
- Powell, D., Grosse-Wilde, E., Krokene, P., Roy, A., Chakraborty, A., Lofstedt, C., et al. (2021). A highly contiguous genome assembly of the Eurasian spruce bark beetle, *Ips typographus*, provides insight into a major forest pest. *Commun. Biol.* 4:1059. doi: 10.1038/s42003-021-02602-3
- Ramakrishnan, R., Hradecky, J., Roy, A., Kalinova, B., Mendezes, R. C., Synek, J., et al. (2022a). Metabolomics and transcriptomics of pheromone biosynthesis in an aggressive forest pest *Ips typographus*. *Insect Biochem. Mol. Biol.* 140:103680. doi: 10.1016/j.ibmb.2021.103680
- Ramakrishnan, R., Roy, A., Kai, M. R., Svatos, A., and Jirosova, A. (2022b). Metabolome and transcriptome related dataset for pheromone biosynthesis in an aggressive forest pest *Ips typographus*. *Data Brief* 41:107912. doi: 10.1016/j.dib.2022.107912
- Rappsilber, J., Mann, M., and Ishihama, Y. (2007). Protocol for micro-purification, enrichment, pre-fractionation and storage of peptides for proteomics using StageTips. *Nat. Protoc.* 2, 1896–1906. doi: 10.1038/nprot.2007.261
- Renwick, J. A. A., Hughes, P. R., and Krull, I. S. (1976). Selective production of *cis-verbenol* and *trans-verbenol* from (–) and (+)- α -pinene by a bark beetle. *Science* 191, 199–201. doi: 10.1126/science.1246609
- Riddiford, L. M. (2012). How does juvenile hormone control insect metamorphosis and reproduction? *Gen. Comp. Endocrinol.* 179, 477–484. doi: 10.1016/j.ygcn.2012.06.001
- Riddiford, L. M., Cherbas, P., and Truman, J. W. (2001). Ecdysone receptors and their biological actions. *Vitamins and Hormones - Advan. Res. App.* 60, 1–73. doi: 10.1016/s0083-6729(00)60016-x
- Riddiford, L. M., Truman, J. W., Mirth, C. K., and Shen, Y. C. (2010). A role for juvenile hormone in the prepupal development of *Drosophila melanogaster*. *Development* 137, 1117–1126. doi: 10.1242/dev.037218
- Rodrigues, T. B., Dhandapani, R., Duan, J., and Palli, S. R. (2017). RNA interference in the Asian Longhorned Beetle: Identification of Key RNAi Genes and Reference Genes for RT-qPCR. *Scientific Reports.* 7:8913. doi: 10.1038/s41598-017-08813-1
- Sandstrom, P., Welch, W. H., Blomquist, G. J., and Tittiger, C. (2006). Functional expression of a bark beetle cytochrome P450 that hydroxylates myrcene to ipsdienol. *Insect Biochem. Mol. Biol.* 36, 835–845. doi: 10.1016/j.ibmb.2006.08.004
- Sarabia, L. E., Lopez, M. F., Obregon-Molina, G., Cano-Ramirez, C., Sanchez-Martinez, G., and Zuniga, G. (2019). The differential expression of mevalonate pathway genes in the gut of the bark beetle *Dendroctonus rhizophagus* (Curculionidae: Scolytinae) is unrelated to the *de novo* synthesis of terpenoid pheromones. *Int. J. Mol. Sci.* 20:20. doi: 10.3390/ijms20164011
- Schlyter, F., Birgersson, G., Byers, J. A., Lofqvist, J., and Bergstrom, G. (1987). Field response of spruce bark beetle, *Ips typographus* to aggregation pheromone candidates. *J. Chem. Ecol.* 13, 701–716. doi: 10.1007/BF01020153
- Sellamuthu, G., Bily, J., Joga, M. R., Synek, J., and Roy, A. (2022). Identifying optimal reference genes for gene expression studies in Eurasian spruce bark beetle, *Ips typographus* (Coleoptera: Curculionidae: Scolytinae). *Sci. Rep.* 12:4671. doi: 10.1038/s41598-022-08434-3
- Seybold, S. J., Quilici, D. R., Tillman, J. A., Vanderwel, D., Wood, D. L., and Blomquist, G. J. (1995). De-novo biosynthesis of the aggregation pheromone components ipsenol and ipsdienol by the pine bark beetles *Ips paraconfusus* lanier and *Ips pini* (say) (Coleoptera: Scolytidae). *Proc. Natl. Acad. Sci. U. S. A.* 92, 8393–8397. doi: 10.1073/pnas.92.18.8393
- Smykal, V., Daimon, T., Kayukawa, T., Takaki, K., Shinoda, T., and Jindra, M. (2014). Importance of juvenile hormone signaling arises with competence of insect larvae to metamorphose. *Dev. Biol.* 390, 221–230. doi: 10.1016/j.ydbio.2014.03.006
- Song, M. M., Kim, A. C., Gorzalski, A. J., MacLean, M., Young, S., Ginzel, M. D., et al. (2013). Functional characterization of myrcene hydroxylases from two geographically distinct *Ips pini* populations. *Insect Biochem. Mol. Biol.* 43, 336–343. doi: 10.1016/j.ibmb.2013.01.003
- Tian, C. B., Li, Y. Y., Huang, J., Chu, W. Q., Wang, Z. Y., and Liu, H. (2020). Comparative transcriptome and proteome analysis of heat acclimation in predatory mite *Neoseiulus barkeri*. *Front. Physiol.* 11:16. doi: 10.3389/fphys.2020.00426
- Tillman, J. A., Holbrook, G. L., Dallara, P. L., Schal, C., Wood, D. L., Blomquist, G. J., et al. (1998). Endocrine regulation of *de novo* aggregation pheromone biosynthesis in the pine engraver, *Ips pini* (say) (Coleoptera: Scolytidae). *Insect Biochem. Mol. Biol.* 28, 705–715. doi: 10.1016/s0965-1748(97)00117-3
- Tillman, J. A., Lu, F., Goddard, L. M., Donaldson, Z. R., Dwinell, S. C., Tittiger, C., et al. (2004). Juvenile hormone regulates *de novo* isoprenoid aggregation pheromone biosynthesis in pine bark beetles, *Ips* spp., through transcriptional control of HMG-CoA reductase. *J. Chem. Ecol.* 30, 2459–2494. doi: 10.1007/s10886-004-7945-z
- Treiblmayr, K., Pascual, N., Piulachs, M.-D., Keller, T., and Belles, X. (2006). Juvenile hormone titer versus juvenile hormone synthesis in female nymphs and adults of the German cockroach, *Blattella germanica*. *J. Insect Sci.* 6, 1–7. doi: 10.1673/031.006.4301
- Trumbo, S. T. (2018). Juvenile hormone and parental care in subsocial insects: implications for the role of juvenile hormone in the evolution of sociality. *Current Opinion in Insect Sci.* 28, 13–18. doi: 10.1016/j.cois.2018.04.001
- Tyanova, S., Temu, T., Sinitcyn, P., Carlson, A., Hein, M. Y., Geiger, T., et al. (2016). The Perseus computational platform for comprehensive analysis of (prote)omics data. *Nat. Methods* 13, 731–740. doi: 10.1038/nmeth.3901
- Ward, S. F., Brockerhoff, E. G., Turner, R. M., Yamanaka, T., Marini, L., Fei, S. L., et al. (2022). Prevalence and drivers of a tree-killing bark beetle, *Ips typographus* (Coleoptera, Scolytinae), in international invasion pathways into the USA. *J. Pest. Sci.* 96, 845–856. doi: 10.1007/s10340-022-01559-4
- White, R. A., Agosin, M., Franklin, R. T., and Webb, J. W. (1980). Bark beetle pheromones - evidence for physiological synthesis mechanisms and their ecological implications. *Zeitschrift Fur Angewandte Entomologie-J. Applied Entomol.* 90, 255–274. doi: 10.1111/j.1439-0418.1980.tb03526.x
- Zhang, W. N., Ma, L., Xiao, H. J., Liu, C., Chen, L., Wu, S. L., et al. (2017). Identification and characterization of genes involving the early step of juvenile hormone pathway in *Helicoverpa armigera*. *Sci. Rep.* 7:16542. doi: 10.1038/s41598-017-16319-z
- Zhu, H., Gegear, R. J., Casselman, A., Kanginakudru, S., and Reppert, S. M. (2009). Defining behavioral and molecular differences between summer and migratory monarch butterflies. *BMC Biol.* 7:14. doi: 10.1186/1741-7007-7-14